



# Higher Atmospheric CO<sub>2</sub> Levels Favor C<sub>3</sub> Plants Over C<sub>4</sub> Plants in Utilizing Ammonium as a Nitrogen Source

Feng Wang<sup>1,2,3\*</sup>, Jingwen Gao<sup>1,3</sup>, Jean W. H. Yong<sup>3,4</sup>, Qiang Wang<sup>1</sup>, Junwei Ma<sup>1\*</sup> and Xinhua He<sup>2,3\*</sup>

<sup>1</sup> Institute of Environmental Resources, Soil and Fertilizer, Zhejiang Academy of Agricultural Sciences, Hangzhou, China, <sup>2</sup> Centre of Excellence for Soil Biology, College of Resources and Environment, Southwest University, Chongqing, China, <sup>3</sup> School of Biological Sciences, The University of Western Australia, Perth, WA, Australia, <sup>4</sup> Department of Biosystems and Technology, Swedish University of Agricultural Sciences, Alnarp, Sweden

## OPEN ACCESS

### Edited by:

Fulai Liu,  
University of Copenhagen, Denmark

### Reviewed by:

Zhaozhong Feng,  
Research Center  
for Eco-environmental Sciences  
(CAS), China  
Xiancan Zhu,  
Anhui Normal University, China  
Xiangnan Li,  
Northeast Institute of Geography  
and Agroecology, Chinese Academy  
of Sciences, China

### \*Correspondence:

Feng Wang  
wangfeng@zaas.ac.cn  
Junwei Ma  
majw@zaas.ac.cn  
Xinhua He  
xinhua.he@uwa.edu.au

### Specialty section:

This article was submitted to  
Plant Nutrition,  
a section of the journal  
Frontiers in Plant Science

**Received:** 24 February 2020

**Accepted:** 05 November 2020

**Published:** 02 December 2020

### Citation:

Wang F, Gao J, Yong JWH,  
Wang Q, Ma J and He X (2020)  
Higher Atmospheric CO<sub>2</sub> Levels Favor  
C<sub>3</sub> Plants Over C<sub>4</sub> Plants in Utilizing  
Ammonium as a Nitrogen Source.  
Front. Plant Sci. 11:537443.  
doi: 10.3389/fpls.2020.537443

Photosynthesis of wheat and maize declined when grown with NH<sub>4</sub><sup>+</sup> as a nitrogen (N) source at ambient CO<sub>2</sub> concentration compared to those grown with a mixture of NO<sub>3</sub><sup>-</sup> and NH<sub>4</sub><sup>+</sup>, or NO<sub>3</sub><sup>-</sup> as the sole N source. Interestingly, these N nutritional physiological responses changed when the atmospheric CO<sub>2</sub> concentration increases. We studied the photosynthetic responses of wheat and maize growing with various N forms at three levels of growth CO<sub>2</sub> levels. Hydroponic experiments were carried out using a C<sub>3</sub> plant (wheat, *Triticum aestivum* L. cv. Chuanmai 58) and a C<sub>4</sub> plant (maize, *Zea mays* L. cv. Zhongdan 808) given three types of N nutrition: sole NO<sub>3</sub><sup>-</sup> (NN), sole NH<sub>4</sub><sup>+</sup> (AN) and a mixture of both NO<sub>3</sub><sup>-</sup> and NH<sub>4</sub><sup>+</sup> (Mix-N). The test plants were grown using custom-built chambers where a continuous and desired atmospheric CO<sub>2</sub> (C<sub>a</sub>) concentration could be maintained: 280 μmol mol<sup>-1</sup> (representing the pre-Industrial Revolution CO<sub>2</sub> concentration of the 18th century), 400 μmol mol<sup>-1</sup> (present level) and 550 μmol mol<sup>-1</sup> (representing the anticipated futuristic concentration in 2050). Under AN, the decrease in net photosynthetic rate (*P<sub>n</sub>*) was attributed to a reduction in the maximum RuBP-regeneration rate, which then caused reductions in the maximum Rubisco-carboxylation rates for both species. Decreases in electron transport rate, reduction of electron flux to the photosynthetic carbon [*Je(PCR)*] and electron flux for photorespiratory carbon oxidation [*Je(PCO)*] were also observed under AN for both species. However, the intercellular (*C<sub>i</sub>*) and chloroplast (*C<sub>c</sub>*) CO<sub>2</sub> concentration increased with increasing atmospheric CO<sub>2</sub> in C<sub>3</sub> wheat but not in C<sub>4</sub> maize, leading to a higher *Je(PCR)/Je(PCO)* ratio. Interestingly, the reduction of *P<sub>n</sub>* under AN was relieved in wheat through higher CO<sub>2</sub> levels, but that was not the case in maize. In conclusion, elevating atmospheric CO<sub>2</sub> concentration increased *C<sub>i</sub>* and *C<sub>c</sub>* in wheat, but not in maize, with enhanced electron fluxes towards photosynthesis, rather than photorespiration, thereby relieving the inhibition of photosynthesis under AN. Our results contributed to a better understanding of NH<sub>4</sub><sup>+</sup> involvement in N nutrition of crops growing under different levels of CO<sub>2</sub>.

**Keywords:** atmospheric CO<sub>2</sub>, ecophysiology, electron transport, NH<sub>4</sub><sup>+</sup> stress, photosynthesis, *Triticum aestivum*, *Zea mays*

## INTRODUCTION

The application of chemical nitrogen (N) fertilizers has greatly increased global crop yields and decreased world hunger over the past five decades (Gong et al., 2011). However, only 30–40 % of applied N is utilized by crops; most is lost in numerous ways, including run-off, leaching, denitrification and volatilization, which together lead to a range of environmental problems (Richter and Roelcke, 2000; Xing and Zhu, 2000). Thus, increasing plant nitrogen use efficiency (NUE) is crucial for the development of sustainable agriculture. Unlike nitrate (NO<sub>3</sub><sup>-</sup>), ammonium (NH<sub>4</sub><sup>+</sup>) can be assimilated by plants without further chemical reduction (Mehrer and Mohr, 1989; Onoda et al., 2004). NH<sub>4</sub><sup>+</sup> can be provided by both manure and urea fertilizers (Xu et al., 2012; Coskun et al., 2017). A promising future strategy for improving agronomic NUE is the application of stabilized-NH<sub>4</sub><sup>+</sup>-based fertilizers together with other active compounds, such as nitrification inhibitors, which can inhibit the nitrification of NH<sub>4</sub><sup>+</sup>, thereby maintaining a high soil N content in the form of NH<sub>4</sub><sup>+</sup> over extended periods (IPCC, 2007; Ariz et al., 2011). Some crops, including wheat and maize, are able to grow well when provided with a mixture of NO<sub>3</sub><sup>-</sup> and NH<sub>4</sub><sup>+</sup> (Mix-N), or NO<sub>3</sub><sup>-</sup> as the sole N source (NN) (Miller and Cramer, 2005). Under certain environmental conditions, NH<sub>4</sub><sup>+</sup> may reduce growth by decreasing photosynthesis, thereby lowering crop productivity (Britto and Kronzucker, 2002). Since urea and NH<sub>4</sub><sup>+</sup>-based N fertilizers are used commonly to support the growth of cereals, vegetables and fruits, a better understanding of the toxic effects of NH<sub>4</sub><sup>+</sup> in plant nutrition should facilitate better crop productivity (Miller and Cramer, 2005; Fernández-Crespo et al., 2012).

Photosynthesis is a synergistic process that involves electron harvesting, transport, and utilization (Kühlbrandt et al., 1994). Photosynthetic electron transport typically involves two reaction centers: photosystems I and II (PSI and PSII, respectively). The D1 protein of PSII is sensitive to NH<sub>4</sub><sup>+</sup>, and a loss of PSII function occurs when NH<sub>4</sub><sup>+</sup>-based fertilizers are applied

in excessive quantities (Drath et al., 2008). When this occurs, impairment of the photosynthetic electron transport chain will lead to a decrease in photochemical efficiency ( $\Phi_{PSII}$ ) and the electron transport rate ( $J_e$ ), in turn leading to a deficiency in NADPH and ATP for CO<sub>2</sub> assimilation (Wang et al., 2019). The atmospheric CO<sub>2</sub> concentration ( $C_a$ ) has increased from 280  $\mu\text{mol mol}^{-1}$  in pre-industrial times to 400  $\mu\text{mol mol}^{-1}$  at present, and is expected to reach 550  $\mu\text{mol mol}^{-1}$  by the 2050 s (IPCC, 2013). The elevation of CO<sub>2</sub> concentration at the sites of Rubisco carboxylation alters plant photosynthetic sensitivity, potentially modulating sensitivity to a diversity of N sources. Due to the importance of food production security and crops in the global carbon cycle, an improved understanding of  $C_a$  changes on the N nutrition of C<sub>3</sub> and C<sub>4</sub> plants will become more and more crucial (Lloyd and Farquhar, 1996; Ghannoum et al., 2000). In general, plants with the C<sub>4</sub> photosynthetic pathway have anatomical and biochemical traits that increase CO<sub>2</sub> levels around the carboxylating Rubisco enzyme (Hatch and Slack, 1966). Bloom et al. (2014) and Dier et al. (2018) showed that NO<sub>3</sub><sup>-</sup> assimilation is inhibited by elevated CO<sub>2</sub> concentrations in field-grown C<sub>3</sub> wheat plants. We postulated that an elevated  $C_a$  increases photosynthesis to produce more carbon skeletons, which in turn would increase NH<sub>4</sub><sup>+</sup> assimilation, thereby ameliorating the possible physiological stress of having excess free NH<sub>4</sub><sup>+</sup> in C<sub>3</sub> plants. The detailed comparative physiological responses of C<sub>3</sub> and C<sub>4</sub> plants to NH<sub>4</sub><sup>+</sup> fertilization under elevated  $C_a$  are still not fully understood (Bloom et al., 2002, 2010; Cousins and Bloom, 2003; Bloom, 2015).

A wide variety of equipment, including open-top chambers (OTC), controlled-environment (CE) systems, and free-air CO<sub>2</sub> enrichment (FACE) systems, has been used to study the effects of elevated  $C_a$ . In the OTC system, plants are held in a chamber with an open top that facilitates gas exchange with the atmosphere (Owensby et al., 1999). However, the temperature is generally higher inside the chamber than outside, inevitably increasing plant transpiration, which influences plant growth rates. The FACE system minimally perturbs the plant growth environment and is suitable for long-term experiments under elevated  $C_a$ . However, the FACE system could not be used to study the effects of sub-ambient CO<sub>2</sub> concentrations. Controlled environment experiments can also be performed in greenhouses and artificial growth chambers (Yong et al., 2000; Aranjuelo et al., 2009; Kanemoto et al., 2009; Robredo et al., 2011). To design a system having minimal impact on natural temperature, light and seasonality, while also having the capacity to provide either sub-ambient or elevated levels of CO<sub>2</sub>, we custom-fabricated experimental chambers in which the inside temperature and humidity were kept similar to outside open field conditions while regulating the  $C_a$ .

Our primary objective was to improve understanding of (i) the physiological mechanisms underlying the photosynthetic inhibition caused by NH<sub>4</sub><sup>+</sup> nutrition and (ii) the mechanism by which  $C_a$  affects the NH<sub>4</sub><sup>+</sup> tolerance of C<sub>3</sub> and C<sub>4</sub> plants. We therefore studied the photosynthetic responses of a C<sub>3</sub> plant (wheat, *Triticum aestivum* L.) and a C<sub>4</sub> plant (maize, *Zea mays* L.). Both these species prefer NO<sub>3</sub><sup>-</sup> as the N nutrient source and we grew them under three  $C_a$  concentrations (280, 400, or 550  $\mu\text{mol mol}^{-1}$ ) combined with three forms of N

Abbreviations:  $\Gamma^*$ , the CO<sub>2</sub> compensation point related to C<sub>i</sub>;  $\phi$ , apparent quantum yield;  $\Phi_{PSII}$ , quantum efficiency of PSII;  $C_a$ , atmospheric CO<sub>2</sub> concentration;  $C_c$ , chloroplast CO<sub>2</sub> concentration; CE, carboxylation efficiency;  $C_i$ , intercellular CO<sub>2</sub> concentration;  $C_m$ , CO<sub>2</sub> concentrations in the mesophyll cells;  $C_s$ , CO<sub>2</sub> concentrations in the bundle sheath; C treatment, the CO<sub>2</sub> concentration treatment of each sample; FACE, free-air CO<sub>2</sub> enrichment;  $F_m$ , the maximum chlorophyll fluorescence with dark-adaptation;  $F_m'$ , the maximum fluorescence with light-adaptation;  $F_o$ , the minimum chlorophyll fluorescence with dark-adaptation;  $F_o'$ , the minimum chlorophyll fluorescence with light-adaptation;  $F_s$ , steady state fluorescence with light-adaptation;  $F_v/F_m$ , maximum quantum efficiency of PSII; gm, mesophyll conductance; gs, stomatal conductance;  $J_a$ , alternative electron flux;  $J_{cmax}$ , maximum carboxylation rates limited by RuBP regeneration;  $J_e(\text{PCO})$ , electron fluxes to photosynthetic carbon oxidation;  $J_e(\text{PCR})$ , electron fluxes to photorespiratory carbon reduction;  $J_{max}$ , maximum electron transport rates; LHC, light-harvesting complex; Mix-N, a mixture of both NO<sub>3</sub><sup>-</sup> and NH<sub>4</sub><sup>+</sup> source; NPQ, non-photochemical quenching; NUE, nitrogen use efficiency; OTC, open-top chambers; Pn, net photosynthetic rate; PPF, photon flux intensity; PSII, photosystem II; PVC, polyvinyl chloride; qL, photochemical quenching; Rd, mitochondrial respiration rate in the light; ROS, reactive oxygen species; Rubisco, ribulose-1,5-bisphosphate carboxylase/oxygenase; vc, the carboxylation rate;  $V_{cmax}$ , maximum carboxylation rate limited by Rubisco; vo, the oxygenation rate; Vpdl, the vapor pressure deficit;  $V_{pmax}$ , the maximal rate of PEP carboxylation; wc, the potential Rubisco carboxylation rate; wj, the potential RuBP regeneration rate; wp, the potential triose-phosphate utilization rate.

nutrition: Mix-N, NN and sole NH<sub>4</sub><sup>+</sup> nitrogen (AN). Our other objective was to provide new knowledge facilitating (i) directed breeding programs aiming to produce N-efficient cultivars, and (ii) the development of sustainable crop N management strategy to adapt to a future with elevated C<sub>a</sub>, as predicted by current models of global climate change.

## MATERIALS AND METHODS

### Plant Materials and Experimental Design

Wheat (*T. aestivum* cv. Chuanmai 58) and maize (*Z. mays* cv. Zhongdan 808), two common crop species in Chongqing, China, were grown under hydroponic experimental conditions. Seeds of both species, of uniform size, were sterilized in 20% (v/v) H<sub>2</sub>O<sub>2</sub> for 10 min, rinsed with distilled water, and germinated in darkness in culture dishes covered with wet sterile gauze. When the cotyledons were 1.0 cm long, the seedlings were transferred to silica sand (previously soaked in 1% HCl for 2 days, followed by flushing with copious amounts of water to remove all traces of HCl) and watered twice daily with distilled water. Uniform 14-day-old (two-leaf stage) seedlings were transplanted into opaque plastic growth containers containing a modified Hoagland's solution (Wang et al., 2016a; Gao et al., 2018), with three N sources: Mix-N, NN or AN. The composition of the Mix-N solution was as follows: macronutrients were provided as 5.0 mM N in the form of Ca(NO<sub>3</sub>)<sub>2</sub>, KNO<sub>3</sub> and (NH<sub>4</sub>)<sub>2</sub>SO<sub>4</sub> (the ratio of NO<sub>3</sub><sup>-</sup> to NH<sub>4</sub><sup>+</sup> in the Mix-N was 3 : 2), 3.0 mM K in the form of KH<sub>2</sub>PO<sub>4</sub> and KNO<sub>3</sub>, 1.5 mM Ca as Ca(NO<sub>3</sub>)<sub>2</sub> and CaCl<sub>2</sub>, 1.0 mM Mg as MgSO<sub>4</sub>, 1.0 mM P as KH<sub>2</sub>PO<sub>4</sub>, and 0.6 mM Na as NaCl. Micronutrients were provided as 0.1 mM Fe as Fe-EDTA, 455 × 10<sup>-3</sup> mM Mn as MnSO<sub>4</sub>, 38.1 × 10<sup>-6</sup> mM Zn as ZnSO<sub>4</sub>, 15.6 × 10<sup>-6</sup> mM Cu as CuSO<sub>4</sub>, 2.31 × 10<sup>-3</sup> mM B as H<sub>3</sub>BO<sub>3</sub>, and 6.2 × 10<sup>-6</sup> mM Mo as MoO<sub>3</sub>. Macronutrients were provided in the NO<sub>3</sub><sup>-</sup>-source solution as 5.0 mM N in the form of Ca(NO<sub>3</sub>)<sub>2</sub> and KNO<sub>3</sub>, 3.0 mM K in the form of KH<sub>2</sub>PO<sub>4</sub> and KNO<sub>3</sub>, 1.5 mM Ca as Ca(NO<sub>3</sub>)<sub>2</sub>, 1.0 mM Mg as MgSO<sub>4</sub>, 1.0 mM P as KH<sub>2</sub>PO<sub>4</sub>, and 0.5 mM Na as NaCl. Macronutrients were provided in the NH<sub>4</sub><sup>+</sup>-source solution as 5.0 mM N in the form of (NH<sub>4</sub>)<sub>2</sub>SO<sub>4</sub>, 3.0 mM K as KH<sub>2</sub>PO<sub>4</sub> and K<sub>2</sub>SO<sub>4</sub>, 1.5 mM Ca as CaCl<sub>2</sub> and CaSO<sub>4</sub>, 1.0 mM Mg as MgSO<sub>4</sub>, 1.0 mM P as KH<sub>2</sub>PO<sub>4</sub>, and 0.5 mM Na as NaCl. Micronutrients in NN or AN source solution were identical to those in the Mix-N source solution; and then kept in chambers (Figure 1A) with the following CO<sub>2</sub> levels: 280 μmol mol<sup>-1</sup> [pre-industrial revolution (i.e., 1840) concentration], 400 μmol mol<sup>-1</sup> (current level), and 550 μmol mol<sup>-1</sup> (projected concentration by the 2050 s) (IPCC, 2013). The temperature and humidity inside the chambers were automatically maintained to match those of the atmosphere outside (Figure 1B). During the night, the CO<sub>2</sub> gradients were held at concentrations 150 ± 1 μmol mol<sup>-1</sup> above daytime levels (Anderson et al., 2001).

A nitrification inhibitor (dicyandiamide, 1 mM) was added to the nutrition solutions to prevent microbial oxidation of NH<sub>4</sub><sup>+</sup>. The pH of the Hoagland's solution was adjusted daily to 5.5 using 0.1 mM NaOH for the plants treated with

NH<sub>4</sub><sup>+</sup>, or with 0.1 mM H<sub>2</sub>SO<sub>4</sub> for those treated with NO<sub>3</sub><sup>-</sup>. The N concentrations were kept constant by replacing the media at 3-day intervals; aeration was provided continuously. We used three CO<sub>2</sub> treatments, with three replicates each in separate chambers (9 chambers in total), and deployed three N treatments for each species in each chamber. Ideally, each experiment should be repeated at least once in every chamber, for each of the planned treatments, to eliminate any intrinsic technical effect of each chamber on plant growth; this represented a potential small shortcoming of the current study in our facility.

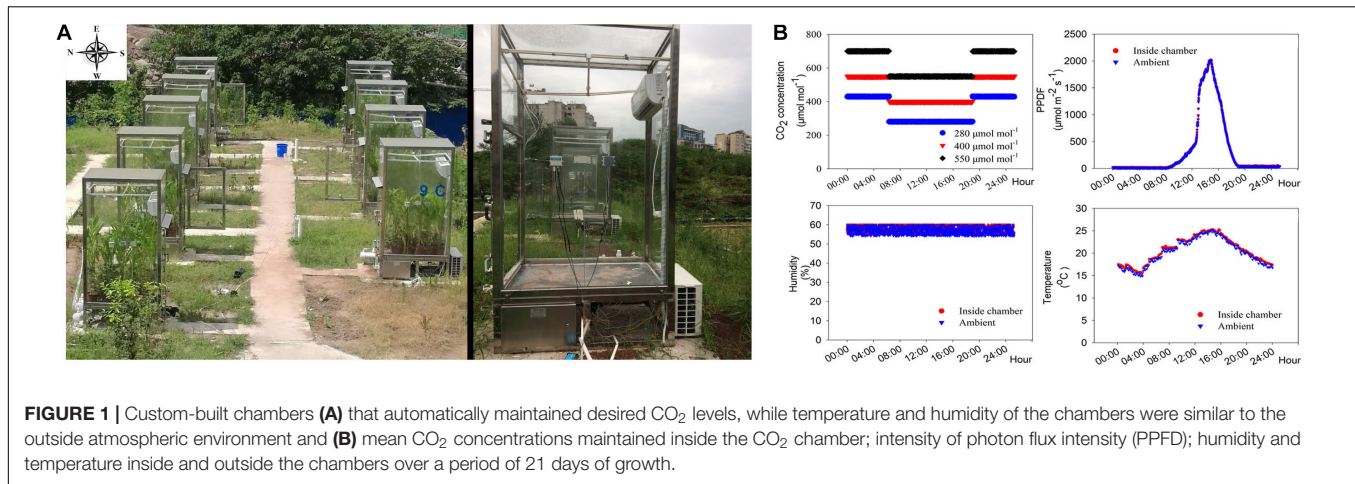
### Experimental Field Chambers

The automatically CE facility consisted of a CO<sub>2</sub> control system (2543CN; Shengsen Corp., Qingdao, China; Supplementary Figures S1-1) and a CO<sub>2</sub> generator (12864; Shengsen Corp.; Supplementary Figure S1-2). The CO<sub>2</sub> generator comprised of several components, i.e., an electric connection point pressure meter (STC90C516RD; Shengsen Corp.), pressure sensors (13864; Shengsen Corp.), and Na<sub>2</sub>CO<sub>3</sub> and H<sub>2</sub>SO<sub>4</sub> feeding inlets (Supplementary Figures S1-5, 6), where the CO<sub>2</sub> was generated according to the following equation: Na<sub>2</sub>CO<sub>3</sub> + H<sub>2</sub>SO<sub>4</sub> = Na<sub>2</sub>SO<sub>4</sub> + H<sub>2</sub>O + CO<sub>2</sub>. The CO<sub>2</sub> generator was connected to the CO<sub>2</sub> control system to maintain the CO<sub>2</sub> concentration in the chambers within a desired set range; CO<sub>2</sub> was delivered through pipes into each chamber.

The chambers were built using toughened glass (10 mm thick, 99% transmittance) walls and roofs (Supplementary Figure S1-13). The floors were covered using a polyvinyl chloride (PVC) material (Supplementary Figure S1-7). Each chamber measured 1,500 × 1,000 × 2,000 mm (length × width × height). CO<sub>2</sub>, temperature and humidity sensors were mounted on both the outer and inner surfaces of the walls (Supplementary Figures S1-8–10). The environmental control mechanism in this system operated automatically and regulated the internal CO<sub>2</sub> concentration (±2.5 μmol mol<sup>-1</sup>), air temperature (±0.5°C) and humidity (±5%) (Figure 1B). The CO<sub>2</sub> control system sensed and assessed the chamber environmental data; these data were later used to regulate the CO<sub>2</sub> injection process and attaining the desired chamber CO<sub>2</sub> levels. When the CO<sub>2</sub> concentration in a chamber exceeded the set concentration, the air was filtered through 1.0 mol mol<sup>-1</sup> NaOH solution using a pump controlled by a mini-computer. When the humidity of a chamber exceeded the set concentration, the air was filtered through dry calcium carbonate using a separate pump controlled by the mini-computer.

### Plant Sampling

The seedlings were sampled between 10:00 and 11:00 at the 21st day of the experiment. Plant organs were separated into two portions: the first was immersed in liquid-N and then stored at -80°C for later chemical analyses, and the second portion was oven-dried at 105°C for 20 min, and then at 75°C for at least 48 hours. The dried material was used later for different chemical analyses. Fresh leaf area was measured using a leaf area scanning device (Li-3000; Li-Cor Inc., Lincoln, NE, United States).



## Gas-exchange Measurements

After 21 days of growth under different N source and CO<sub>2</sub> level conditions, we measured gas exchange and chlorophyll fluorescence simultaneously on the first fully developed leaves during the morning (09:00–11:00) using a Li-Cor 6400 infrared gas analyzer (Li-Cor 6400; Li-Cor Inc.). The leaf temperature during measurements was maintained at  $25.0 \pm 0.5^\circ\text{C}$ . Leaves were illuminated with a steady red and blue light source at a photosynthetic photon flux density (PPFD) of  $1,500 \mu\text{mol m}^{-2} \text{s}^{-1}$  (Yong et al., 2000, 2010). The reference CO<sub>2</sub> concentrations in the cuvettes matched the treatment CO<sub>2</sub> concentrations to which samples had been previously subjected ( $C_{\text{treatment}}$ ), i.e.,  $280 \pm 2.5$ ,  $400 \pm 2.5$  or  $550 \pm 2.5 \mu\text{mol mol}^{-1}$ . The vapor pressure deficit (Vpdl) was  $1.1 \pm 0.05 \text{ kPa}$ , and the relative humidity was in the range 55–65%. The gas exchange instrument was calibrated each day before the measurements and matched at least twice a day (between the curves). Data were recorded after sample acclimation in the cuvette for at least 15 min.

Two types of curves were plotted: net photosynthesis ( $A_n$ ) vs. intercellular CO<sub>2</sub> concentrations ( $C_i$ , **Supplementary Figure S2**), and  $A_n$  vs. PPFDF. Simultaneous measurements of chlorophyll fluorescence and parameters for plotting the  $A/C_i$  curves were made on the same leaf using the Li-Cor 6400 infrared gas analyzer. Leaf temperature, PPFDF, Vpdl and relative humidity were maintained as indicated above. Prior to measurement, leaves were held in the cuvette at a reference CO<sub>2</sub> concentration of  $C_{\text{treatment}}$  for at least 10 min. The reference CO<sub>2</sub> concentration was controlled across a series of  $C_{\text{treatment}}$  values: 200, 150, 100, 50, 400, 600, 800, 1,000, 1,200, and  $1,500 \mu\text{mol mol}^{-1}$ . Data were collected after the prevailing CO<sub>2</sub> had reached a steady state (2–3 min).

## Method for Determining Photosynthetic Parameters of C<sub>3</sub> and C<sub>4</sub> Plants

The parameters for the C<sub>3</sub> wheat plant photosynthesis model were calculated using the equations of Farquhar et al. (1980); Long and Bernacchi (2003), Gao et al. (2018), and Wang et al. (2019).

According to the photosynthesis model that we used for C<sub>4</sub> maize plants (von Caemmerer and Farquhar, 1999), the rates of phosphoenolpyruvate (PEP) and Rubisco carboxylation ( $V_p$  and  $V_c$ , respectively) are the major determinants of the net CO<sub>2</sub> assimilation rate. The Rubisco carboxylation rate ( $V_{cmax}$ ), the maximal rate of PEP carboxylation ( $V_{pmax}$ ), maximum RuBP-regeneration rate ( $J_{max}$ ) and CO<sub>2</sub> concentration in the bundle sheath ( $C_s$ ) for maize were calculated using the following equations. The photosynthetic rate was expressed mathematically as:

$$A = V_p - R_m - L \quad (1)$$

and

$$A = V_c - 0.5V_0 - R_d \quad (2)$$

where  $R_m$  is the mitochondrial respiration of the mesophyll cells,  $L$  is the rate of CO<sub>2</sub> leakage from the bundle sheath into the mesophyll, and  $R_d$  is the mitochondrial respiration rate in the light.

$$L = g_{bs} \times (C_s - C_m) \quad (3)$$

$$C_m = C_i - \frac{A}{g_i} \quad (4)$$

where  $g_{bs}$  is the bundle sheath conductance for CO<sub>2</sub>,  $g_i$  is the mesophyll conductance for CO<sub>2</sub>,  $C_s$  is the CO<sub>2</sub> concentration in the bundle sheath, and  $C_m$  is the CO<sub>2</sub> concentration in the mesophyll cells.  $V_0$  is the rate of Rubisco oxygenation:

$$V_0 = \frac{2\gamma^* O}{C_s} \times V_c \quad (5)$$

where  $\gamma^*$  is one half of the reciprocal of Rubisco specificity ( $S_{c/o}$ ), and  $O$  is the oxygen concentration in the bundle sheath cells, which matches the oxygen concentration in the mesophyll cells. By fitting equation (3) to equation (1), and equation (5) to equation (2), we obtained the following expressions:

$$A = V_p - R_m - g_{bs} \times (C_s - C_m) \quad (6)$$

and

$$A = V_c \times \left(1 - \frac{\gamma^* O}{C_s}\right) - R_d \quad (7)$$

$V_p$  and  $V_c$  depend on  $V_{cmax}$ ,  $V_{pmax}$ ,  $J_{max}$ , the Michaelis constants for O<sub>2</sub> and CO<sub>2</sub> ( $K_o$ ,  $K_c$  and  $K_p$ ), and the relative specificity of Rubisco ( $S_{c/o}$ ).

To calculate  $V_{cmax}$  and  $V_{pmax}$ , we used the enzyme-limited expressions of  $V_p$  and  $V_c$ :

$$V_p = \frac{C_m V_{pmax}}{C_m + K_p} \quad (8)$$

$$V_c = \frac{C_s V_{cmax}}{C_s + K_p \left(1 + \frac{O}{K_o}\right)} \quad (9)$$

By fitting equation (8) to equation (6), and equation (9) to equation (7), we obtained the following expressions:

$$A = \frac{C_m V_{pmax}}{C_m + K_p} - R_m - g_{bs} \times (C_s - C_m) \quad (10)$$

and

$$A = \frac{C_s V_{cmax}}{C_s + K_c \left(1 + \frac{O}{K_o}\right)} \times \left(1 - \frac{\gamma^* O}{C_s}\right) - R_d \quad (11)$$

In equations (4), (10) and (11),  $g_i$ ,  $g_{bs}$ ,  $R_m$ ,  $K_p$ ,  $K_c$ ,  $K_o$ ,  $O$ ,  $R_d$  and  $\gamma^*$  were constant parameters at a given temperature [as described by von Caemmerer and Farquhar (1999)],  $A$  and  $C_i$  were measured values, and  $C_m$ ,  $C_s$ ,  $V_{cmax}$  and  $V_{pmax}$  were unknowns. Two pairs of ( $A$ ,  $C_i$ ) (with  $C_i$  limited to 40–80  $\mu\text{mol mol}^{-1}$ ) were then inserted into two sets of equations (5), (8) and (9), following which we obtained six equations and six unknowns ( $V_{cmax}$ ,  $V_{pmax}$ ,  $C_s1$ ,  $C_s2$ ,  $C_m1$  and  $C_m2$ ) using the Matlab software (MathWorks, Natick, MA, United States).

To calculate  $J_{max}$ , we used the electron transport limited expressions of  $V_p$  and  $V_c$ :

$$V_p = \frac{xJ_t}{2} \quad (12)$$

$$V_c = \frac{(1-x)J_t}{3 \left(1 + \frac{7\gamma^* O}{3C_s}\right)} \quad (13)$$

where  $x$  is a partitioning factor of electron transport, and  $J_t$  is the electron transport rate, given by:

$$J_t = \frac{I_2 + J_{max} - \sqrt{(I_2 + J_{max})^2 - 4\theta I_2 J_{max}}}{2\theta} \quad (14)$$

where  $I_2$  is the total absorbed irradiance, which is a function of the incident irradiance  $I$ , and  $\theta$  is an empirical curvature factor.

By fitting equation (11) to equation (6), and equation (12) to equation (7), we obtained:

$$A = \frac{xJ_t}{2} - R_m - g_{bs} \times (C_s - C_m) \quad (15)$$

and

$$A = \frac{(1-x)J_t}{3 \left(1 + \frac{7\gamma^* O}{3C_s}\right)} - R_d \quad (16)$$

$C_m$  was obtained from equation (4). In equations (15) and (16),  $x$  and  $\gamma^*$  are constants at a given temperature,  $A$ ,  $C_m$  and  $I$  (PPFD) are known values, and  $J_{max}$  and  $C_s$  are unknown entities. With two equations and two unknowns, and incorporating the single values of  $A$  and  $I$  (PPFD), we obtained the values for  $J_{max}$  and  $C_s$ .

## Chlorophyll Fluorescence Measurements

Light adapted chlorophyll fluorescence was measured with a Li-Cor 6400 infrared gas analyzer while simultaneously measuring gas exchange, as described above. Steady-state fluorescence ( $F_s$ ) was measured under actinic light. A saturating light pulse ( $\sim 8,000 \mu\text{mol photons m}^{-2} \text{s}^{-1}$ ) was applied for 0.7 s to obtain the maximum fluorescence ( $F_m'$ ). After removing the actinic light and applying 3 s of far-red light, the minimal fluorescence of the light-adapted state ( $F_o'$ ) was obtained. The quantum efficiency of PSII ( $\Phi_{PSII}$ ) and  $J_t$  were calculated using equations (17) and (18), respectively, following Genty et al. (1989) and Li et al. (2009):

$$\Phi_{PSII} = \frac{F_m' - F_s}{F_m'} \quad (17)$$

$$J_t = \frac{F_m' - F_s}{F_m'} \times \text{PPFD} \times 0.85 \times 0.5 \quad (18)$$

The central portion of the same leaf ( $\sim 70\%$  leaf area) was chosen for measurement of dark-adapted and light-adapted chlorophyll fluorescence parameters using a Fluor imager (CF Imager; Technologia Ltd., Colchester, United Kingdom). The minimum and maximum chlorophyll fluorescence ( $F_o$  and  $F_m$ , respectively) values were determined after full dark adaptation for at least 30 min.  $F_s$ ,  $F_m'$ , and  $F_o'$  were obtained as described above. The maximum quantum efficiency of PSII ( $F_v/F_m$ ) was calculated using equation (32) of Genty et al. (1989):

$$F_v/F_m = \frac{F_m - F_o}{F_m} \quad (19)$$

Photochemical quenching ( $qL$ ) was calculated using equation (20) and non-photochemical quenching (NPQ) was calculated using equation (21), following Kramer et al. (2004).

$$qL = \frac{F_o'}{F_s} \times \frac{F_m' - F_s}{F_m' - F_o'} \quad (20)$$

$$\text{NPQ} = \frac{F_m - F_m'}{F_m'} \quad (21)$$

## Calculating Electron Flux to the Photosynthetic Carbon Reduction Cycle [Je(PCR)], and Electron Flux to the Photorespiratory Carbon Oxidation Cycle [Je(PCO)]

The  $J_t$  in the photosynthetic carbon reduction and photorespiratory carbon oxidation cycles were expressed as

follows (Zhou et al., 2004):

$$Je(PCR) = 4 \times v_c = 4 \times \frac{A + R_d}{1 - \frac{\Gamma^*}{C_i}} \quad (22)$$

$$Je(PCO) = 4 \times v_o \quad (23)$$

## Determination of Free NH<sub>4</sub><sup>+</sup> and Soluble Sugar Concentrations

The free NH<sub>4</sub><sup>+</sup> in plant tissues was determined according to Balkos et al. (2010) with some modifications. Briefly, plant tissues were desorbed in 10 mM CaSO<sub>4</sub> for 5 min, and then rinsed with deionized water to remove any extracellular NH<sub>4</sub><sup>+</sup>. Approximately 0.5 g of fresh material was homogenized with liquid nitrogen; NH<sub>4</sub><sup>+</sup> was then extracted in 5 ml of 10 mM formic acid. Supernatants were collected after centrifugation at 10,000 g (4°C) for 15 min, transferred to 5-ml polypropylene tubes after filtration through 0.45-μm organic ultra-filtration membranes, and re-centrifuged at 50,000 g (4°C) for 10 min. An *O*-phthalaldehyde (OPA) reagent was prepared by combining 200 mM potassium phosphate buffer (equimolar amounts of potassium dihydrogen phosphate and potassium monohydrogen phosphate), 3.75 mM OPA, and 2 mM 2-mercaptoethanol (v/v/v = 1:1:1). Prior to adding 2-mercaptoethanol, the pH was adjusted to 7.0 using 1 M NaOH, and the solution was then filtered through two layers of filter paper. A 10-μl aliquot of tissue extract was mixed with 3 ml of OPA reagent. The color was developed in darkness at 25°C for 30 min before carrying out absorbance measurements at 410 nm using a spectrophotometer (model UV-2401, Shimadzu Corp., Kyoto, Japan).

Soluble sugar concentrations were measured following the method of Wang et al. (2016a). Dry powdered shoot and root samples (0.5 g) were extracted in 80% (v/v) ethanol at 80°C for 30 min. The extracts were later centrifuged at 3000 g for 10 min and the supernatants were collected. This extraction procedure was repeated three times to ensure all soluble sugars were extracted. The supernatants were evaporated on china dishes in a hot water bath. Residues were then re-dissolved in 1-3 ml of distilled water and filtered through 0.4-μm film to assay soluble sugars. Concentrations of soluble sugar were measured using the anthrone method. Anthrone sulfuric acid (5 ml) solution (75% v/v) was added to 0.1 ml of supernatant and heated to 90°C for 15 min. Absorbance at 620 nm was measured using a spectrophotometer (model UV-2401, Shimadzu Corp., Kyoto, Japan).

## Statistical Analysis

We found significant effects of N forms (Mix-N, NN, AN) and CO<sub>2</sub> levels on the measured parameters in wheat and maize using the two-way ANOVA ( $P < 0.05$ ,  $n = 3$ ). Significant pairwise differences between means were identified with Dunnett's multiple comparisons test ( $P < 0.05$ ). The proportion of variation (%) explainable by each factor was estimated as the total sums of squares. Calculations were performed with SPSS software (SPSS, Inc., Chicago, United States). Graphs were plotted

using SigmaPlot 10.0 software (Systat Software, Inc., Chicago, IL, United States).

## RESULTS

### Dry Biomass, Leaf Area and Free NH<sub>4</sub><sup>+</sup>

Compared with the Mix-N treatment, AN significantly reduced the shoot and root biomass of both wheat and maize plants (Figure 2). However, with increasing CO<sub>2</sub> concentration, wheat shoot and root biomass increased significantly, although these biomass parameters did not differ significantly according to CO<sub>2</sub> levels in maize. Shoot biomass in wheat under AN was reduced by 38%, 27%, and 14% at CO<sub>2</sub> concentrations of 280, 400 and 550 μmol mol<sup>-1</sup>, respectively (in comparison with the Mix-N treatment). The decreases were larger in maize (46%, 44% and 44% at CO<sub>2</sub> concentrations of 280, 400, or 550 μmol mol<sup>-1</sup>, respectively) (Figure 2). The AN treatment reduced the total leaf area, where the reduction was again greater in maize than in wheat. With increasing CO<sub>2</sub> concentrations, the total foliage area of wheat increased significantly, but this was not the case for maize. Free NH<sub>4</sub><sup>+</sup> concentrations did not differ significantly in either species between the Mix-N and NN treatments with increasing CO<sub>2</sub> concentration (Figure 2) whereas, in comparison with the other two treatments, the AN increased free NH<sub>4</sub><sup>+</sup> in shoots and roots. The concentration of free NH<sub>4</sub><sup>+</sup> decreased significantly with increasing CO<sub>2</sub> concentration in wheat, but not in maize.

Only the N form had significant effects on maize shoot dry biomass; in wheat, the N form, CO<sub>2</sub> level, and their interaction significantly affected shoot biomass (Table 1). Changes in CO<sub>2</sub> levels caused a higher proportion of the variance in wheat shoot dry biomass than did changes in N form. Total leaf area in the two species was significantly affected by both N form and CO<sub>2</sub> level. N form explained a larger proportion of the variance in total leaf area in both species. Alterations in CO<sub>2</sub> levels explained a much greater proportion of the variance in total leaf area variation in wheat (38%) than in maize (0.5%). In both species, the quantity of free NH<sub>4</sub><sup>+</sup> in shoots and roots differed significantly according to the form of N supplied. Interestingly, the CO<sub>2</sub> level had significant effects on free NH<sub>4</sub><sup>+</sup> in tissues of wheat, but not in maize.

### Photosynthesis and Its Related Parameters

Compared with Mix-N and NN, AN treatment reduced the net photosynthetic rate ( $P_n$ ) of both maize and wheat, although the effect was greater in the former species (Figure 3). The  $P_n$  of wheat plants growing under 550 μmol CO<sub>2</sub> mol<sup>-1</sup> was significantly higher than that of plants grown under 280 and 400 μmol CO<sub>2</sub> mol<sup>-1</sup>. Conversely, the  $P_n$  of maize plants under AN did not differ significantly according to the CO<sub>2</sub> level. On day 21 of the experiment, the  $P_n$  of maize under AN was reduced in comparison with those under the Mix-N treatment, by 34%, 32% and 32% at CO<sub>2</sub> concentrations of 280, 400, and 550 μmol mol<sup>-1</sup>, respectively. The respective reductions in wheat were 30%, 27% and 19%.

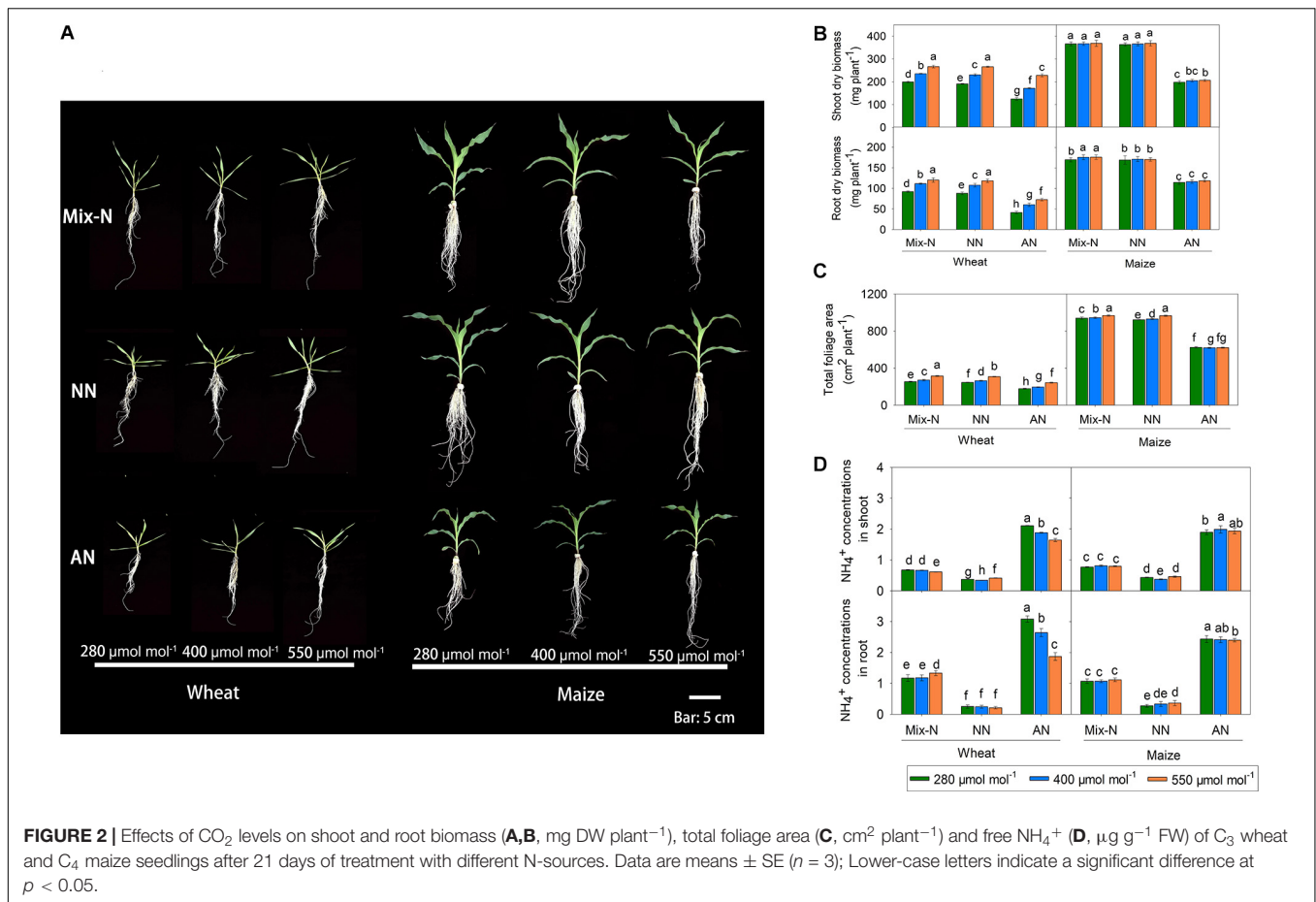


**TABLE 1 |** F-values in two-way ANOVA analysis of biomass, total foliage area and free NH<sub>4</sub><sup>+</sup> in newly expanded leaves of C<sub>3</sub> wheat and C<sub>4</sub> maize seedlings after 21 days of treatment with different N-sources.

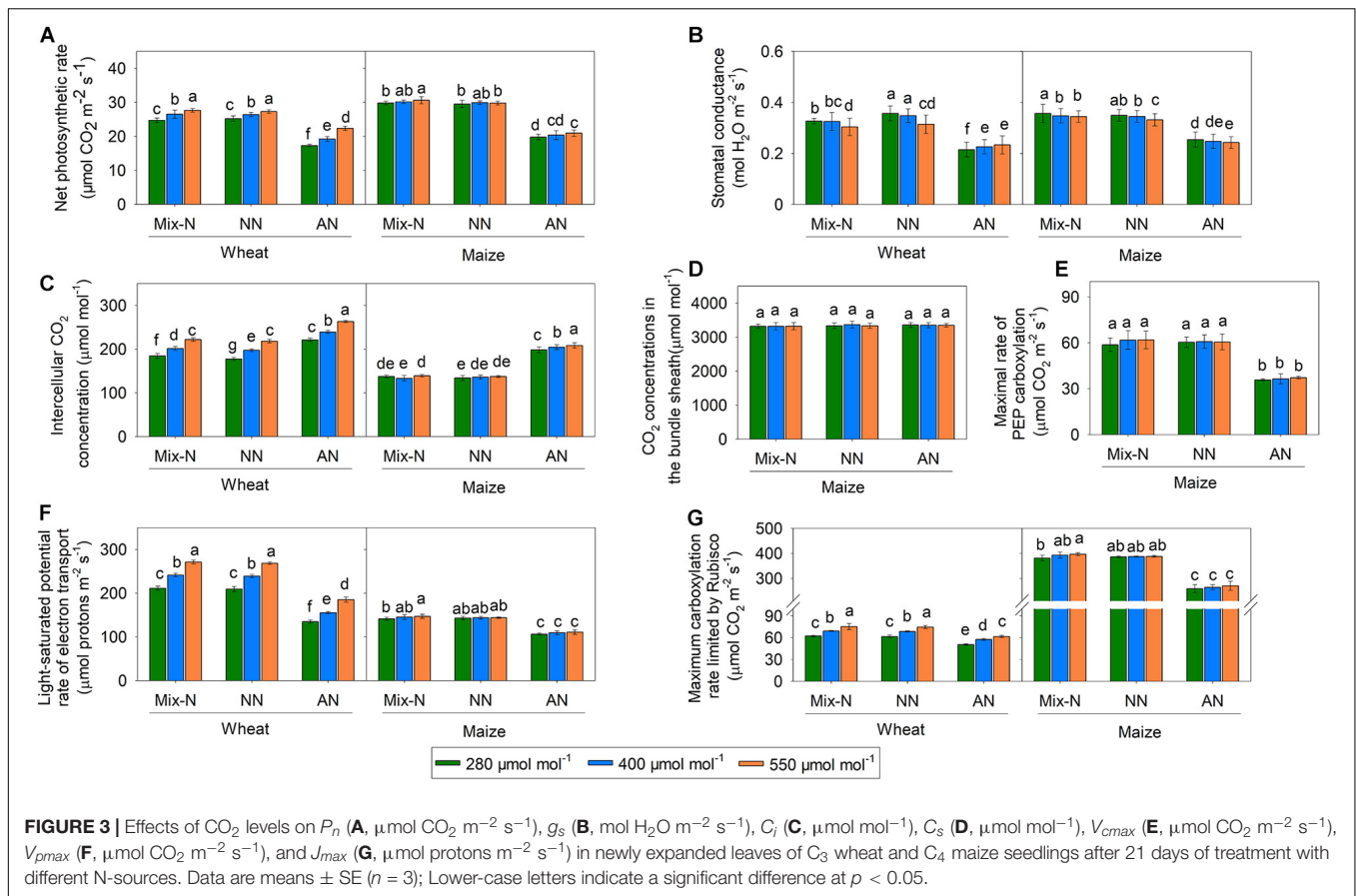
Species	N-form	CO <sub>2</sub> level	Shoot dry weight		Root dry weight		Total foliage area		Free NH <sub>4</sub> <sup>+</sup> in shoot		Free NH <sub>4</sub> <sup>+</sup> in root	
Species	Source	df	Squares sum (×10 <sup>3</sup> )	F-value	Squares sum (×10 <sup>2</sup> )	F-value	Squares sum (×10 <sup>3</sup> )	F-value	Squares sum	F-value (×10 <sup>2</sup> )	Squares sum	F-value (×10 <sup>2</sup> )
Wheat	N	2	38.8(38.1)	2758**	279.8(76.5)	1822**	61(61.2)	1824**	23.09(97.1)	337.6**	47.6(91.0)	115.0**
	CO <sub>2</sub>	2	60.5(59.4)	4302**	82.8(22.6)	539**	38(38.1)	1134**	0.24(1.0)	3.5**	1.2(5.3)	2.9**
	N × CO <sub>2</sub>	4	2.3(2.3)	83**	0.3(0.1)	1 ns	0 (0.0)	1 ns	0.40(1.9)	3.3**	3.4(15.1)	4.1**
	Error	40	0.3(0.3)		3.1(0.8)		1(0.7)		0.01(0.1)		0.1(0.4)	
Maize	N	2	321.2(99.3)	3445.6**	372.4(97.9)	1279**	1258(99.2)	42843**	22.50(99.3)	48.0**	40.0(99.6)	71.9**
	CO <sub>2</sub>	2	0.3(0.08)	2.7 ns	1.6(0.4)	5**	6(0.5)	197**	0.01(0.0)	0.0 ns	0.0(0.0)	0.0
	N × CO <sub>2</sub>	4	0.1(0.03)	0.5 ns	0.6(0.1)	1 ns	4(0.3)	61**	0.04(0.2)	0.1**	0.0(0.2)	0.0
	Error	40	1.9(0.58)		5.8(1.5)		1(0.0)		0.09(0.4)		0.1(0.5)	

N refers to the three nitrogen-forms effect; CO<sub>2</sub> refers to the three CO<sub>2</sub> levels effect; N × CO<sub>2</sub> refers to nitrogen-form × CO<sub>2</sub> levels interaction effects. Values in brackets following the sum of squares for variables indicate the percentage (%) of given variation to total variation. \*\* indicate significant at 0.01 level, respectively. df refers to the degree of freedom. ns means no significant difference.

The *g<sub>s</sub>* values did not differ significantly by CO<sub>2</sub> concentration, but were significantly reduced by AN treatment compared with the other two treatments, in both species (Figure 3). *C<sub>i</sub>* increased significantly with increasing CO<sub>2</sub> concentration in wheat, but not in maize. The AN treatment significantly increased *C<sub>i</sub>* in both species in comparison with the other two treatments. On day 21 of the experiment, we found no significant differences

in C<sub>s</sub> according to either the treatment or CO<sub>2</sub> concentration. *V<sub>pmax</sub>* did not vary significantly by CO<sub>2</sub> concentration, but was significantly reduced under AN in comparison with the other two treatments.

The *V<sub>cmax</sub>* and *J<sub>max</sub>* of wheat increased significantly with increasing CO<sub>2</sub> concentration within the same level of the N form factor, but this was not the case for maize (Figure 3).



In comparison with the other two treatments, AN reduced  $V_{cmax}$  and  $J_{max}$  in both species. The reduction in  $V_{cmax}$  associated with AN was larger in maize than in wheat, while the reduction in  $J_{max}$  was smaller in maize than in wheat. On day 21 of the experiment, AN reduced  $V_{cmax}$  in maize in comparison with Mix-N, by 32%, 33% and 32% at CO<sub>2</sub> concentrations of 280, 400, and 550  $\mu\text{mol mol}^{-1}$ , respectively. The respective reductions in wheat were 19%, 17%, and 18%. Moreover, AN reduced the  $J_{max}$  of maize in comparison with Mix-N, by 25%, 25%, and 24% at CO<sub>2</sub> concentrations of 280, 400, and 550  $\mu\text{mol mol}^{-1}$ , respectively. The respective reductions in wheat were 36%, 36%, and 32%.

The  $P_n$ ,  $g_s$ ,  $C_i$ ,  $V_{cmax}$  and  $J_{max}$  varied significantly according to both the N treatment type and the CO<sub>2</sub> level. The N form accounted for a larger proportion of the variance in these parameters in both species (Table 2). The effect of CO<sub>2</sub> level was much greater in wheat than in maize. The  $V_{pmax}$  of maize was significantly affected only by the N form. The  $C_s$  in maize was not affected by the N form, CO<sub>2</sub> level, or their interaction, nor by the interaction between pH and the N form.

## Electron Transport Parameters

Under Mix-N and NN, the  $F_v/F_m$ ,  $\Phi_{PSII}$  and  $qL$  values of the two species did not vary significantly across different CO<sub>2</sub> concentration (Figures 4A–C). The values of these parameters decreased with increasing CO<sub>2</sub> concentration in maize plants

under AN, but increased in wheat plants as CO<sub>2</sub> concentrations rose. NPQ increased significantly under AN in comparison with the other treatments, but did not differ significantly by CO<sub>2</sub> level (Figure 4D). The  $F_v/F_m$ ,  $\Phi_{PSII}$  and  $qL$  values of wheat varied significantly by both N form and CO<sub>2</sub> concentration, as observed for  $\Phi_{PSII}$  and  $qL$  in maize (but not for  $F_v/F_m$ ). N form explained a larger proportion of the variance in these parameters in both species than CO<sub>2</sub> concentration (Table 3). CO<sub>2</sub> level accounted for a larger proportion of the variance in electron transport in wheat (8.9% for  $F_v/F_m$ , 5.1% for  $\Phi_{PSII}$  and 5.5% for  $qL$ ) than in maize (0.0% for  $F_v/F_m$ , 0.5% for  $\Phi_{PSII}$  and 0.4% for  $qL$ ).

Under Mix-N and NN, the values of  $J_t$  for both species did not differ significantly across different CO<sub>2</sub> concentration (Figure 5A). However, while the values of  $J_t$  for wheat plants under AN increased significantly with increasing CO<sub>2</sub> concentration, this was not the case for maize. On day 21 of the experiment, AN reduced the  $J_t$  values to below those of plants under Mix-N, by 31%, 32% and 32% in maize at CO<sub>2</sub> concentrations of 280, 400, or 550  $\mu\text{mol mol}^{-1}$ , respectively. The respective reductions in wheat were 38%, 30%, and 21%. The  $Je(PCR)$  values of wheat were higher under CO<sub>2</sub> concentrations of 400 and 550  $\mu\text{mol mol}^{-1}$  than under a concentration of 280  $\mu\text{mol mol}^{-1}$ . CO<sub>2</sub> level had no significant effect on the  $Je(PCR)$  values of maize (Figure 5B). In comparison with the other treatments, AN significantly reduced  $Je(PCR)$  in both species. Under AN, the  $Je(PCR)$  values of wheat increased



**TABLE 2** | F-values in two-way ANOVA analysis of  $P_n$ ,  $g_s$ ,  $C_i$ ,  $C_s$ ,  $V_{cmax}$ ,  $V_{pmax}$ , and  $J_{max}$  in newly expanded leaves of C<sub>3</sub> wheat and C<sub>4</sub> maize seedlings after 21 days of treatment with different N-sources.

Species	N-form	CO <sub>2</sub> level	$P_n$	$g_s$	$C_i$	$C_s$	$V_{cmax}$	$V_{pmax}$	$J_{max}$
Species	Source	df	Squares sum ( $\times 10^3$ )	F-value	Squares sum ( $\times 10^3$ )	F-value	Squares sum ( $\times 10^3$ )	Squares sum ( $\times 10^2$ )	Squares sum ( $\times 10^3$ )
Wheat	N	2	532(80.7)	1217**	205.0(57.7)	2758**	1.75(53.7)	273**	80.1(73.0)
	CO <sub>2</sub>	2	102(15.4)	232**	145.3(40.9)	4302**	1.38(42.1)	214**	28.7(26.1)
	N $\times$ CO <sub>2</sub>	4	17(2.5)	18*	0.4(0.1)	83**	0.01(0.3)	1 ns	0.2(0.2)
	Error	40	9(1.3)	4(2.7)	4.7(1.3)	0.13(3.9)			0.7(0.6)
Maize	N	2	1108(98.3)	1647**	546.3(98.4)	2396**	184.7(97.0)	826**	14.9(94.9)
	CO <sub>2</sub>	2	5(0.4)	7**	2.4(0.4)	10**	0.9(0.5)	4*	0.1(0.9)
	N $\times$ CO <sub>2</sub>	4	1(0.1)	1 ns	2.0(0.4)	4**	0.3(0.2)	1 ns	0.0(0.3)
	Error	40	13(1.2)	2(1.7)	4.6(0.8)	2987(95.3)	4.5(2.3)	5.5(7.3)	0.6(4.0)

N refers to the three nitrogen-forms effect; CO<sub>2</sub> refers to the three CO<sub>2</sub> levels effect; N  $\times$  CO<sub>2</sub> refers to nitrogen-form  $\times$  CO<sub>2</sub> levels interaction effects. Values in brackets following the sum of squares for variables indicate the percentage (%) of given variation to total variation. \* and \*\* indicate significant at 0.05 and 0.01 level, respectively. df refers to the degree of freedom. ns means no significant difference.

significantly with increasing CO<sub>2</sub> concentration, but this was not the case for maize. When compared to other N form treatments, AN significantly reduced  $Je(PCO)$  in both species (**Figure 5C**) on day 21 of the experiment. The  $Je(PCR)/Je(PCO)$  ratio increased significantly with increasing CO<sub>2</sub> concentration in wheat. The ratio in maize was unaffected by either CO<sub>2</sub> level or N form (**Figure 5D**).

$J_t$ ,  $Je(PCR)$ ,  $Je(PCO)$  and the  $Je(PCR)/Je(PCO)$  ratio were significantly affected by N form and CO<sub>2</sub> level in both species. N form explained a larger proportion of the variance in these parameters in both species (**Table 4**). In wheat, 40% of the variance in the  $Je(PCR)/Je(PCO)$  ratio could be attributed to CO<sub>2</sub> level, but this factor accounted for only 2.9% of the variance in maize (**Table 4**).

## Soluble Sugars

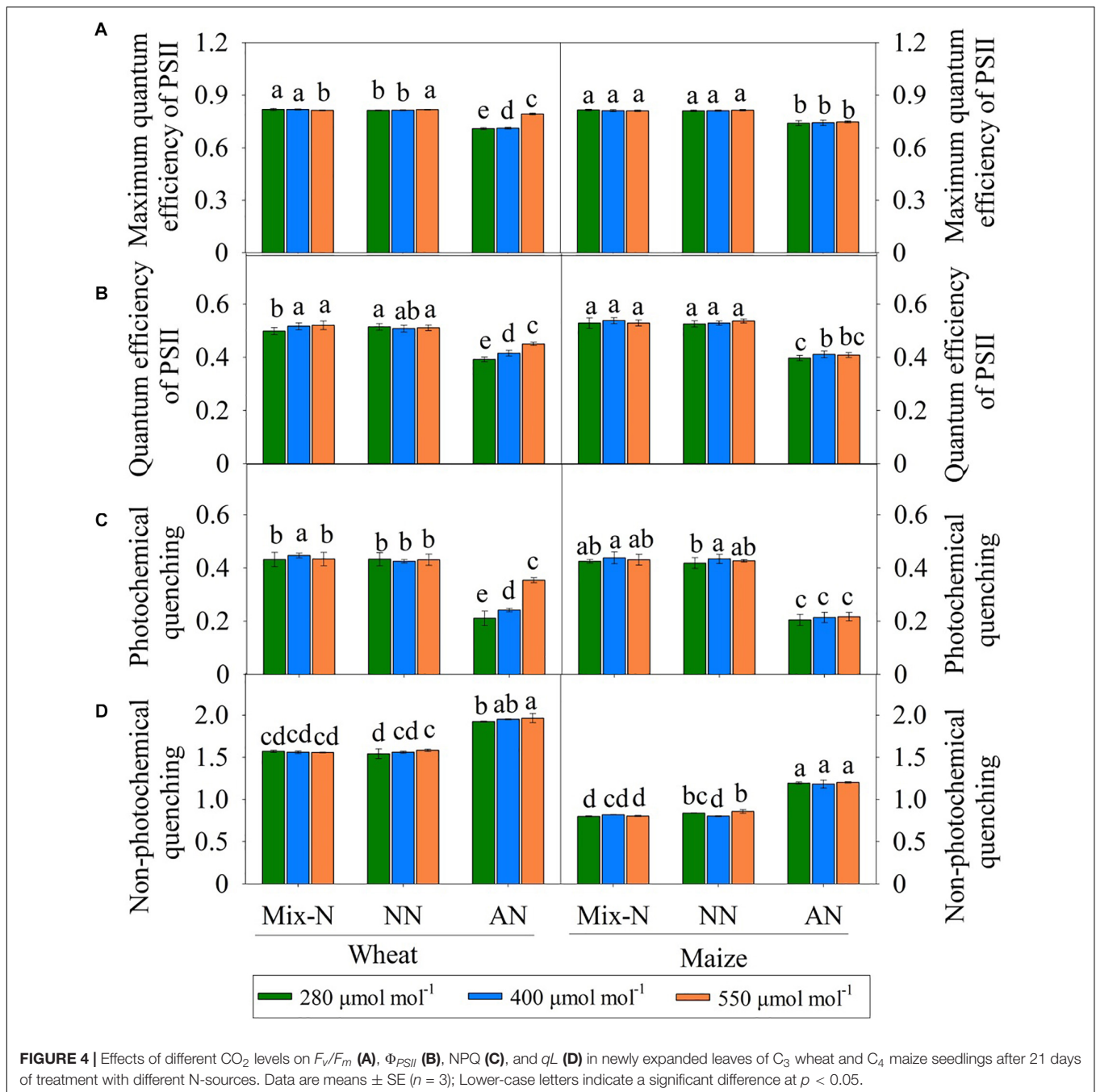
In comparison with the other N form treatments, AN markedly reduced the soluble sugar concentration in both species. Soluble sugar levels in the shoots and roots of wheat increased with increasing CO<sub>2</sub> concentration, but this was not the case in maize (**Figure 6**).

## DISCUSSION

### Increased Atmospheric CO<sub>2</sub> Concentrations Offset NH<sub>4</sub><sup>+</sup>-Linked Stress in C<sub>3</sub> Wheat but Not in C<sub>4</sub> Maize

Unlike field or pot experiments, hydroponic experiments remove any potential complex interaction between ions and soil particles that might affect nutrient availability, and thus plant growth and development (Conn et al., 2013; Nguyen et al., 2016). We harnessed the hydroponic approach to study the responses of C<sub>3</sub> wheat and C<sub>4</sub> maize to different N forms and three levels of CO<sub>2</sub> concentrations. In previous studies, the most obvious effect of AN was reduced biomass production (Britto and Kronzucker, 2002; Li et al., 2011; Wang et al., 2016b, 2019). In the present study, the Mix-N and NO<sub>3</sub><sup>-</sup>-fed C<sub>3</sub> wheat plants produced more dry biomass when the corresponding C<sub>a</sub> concentration was increased, but this was not the case for C<sub>4</sub> maize, corroborating the findings of Leakey et al. (2006). When C<sub>a</sub> was low, the leaf-free NH<sub>4</sub><sup>+</sup> content was highest in C<sub>4</sub> maize with NH<sub>4</sub><sup>+</sup> as the sole N source (**Figure 2**); concomitantly under these conditions, we recorded the lowest  $P_n$  values for maize (**Figure 3**).

In C<sub>3</sub> wheat, AN-induced photosynthetic inhibition was ameliorated by increasing the C<sub>a</sub> concentration, but this effect was insignificant in C<sub>4</sub> maize (**Figure 3**). Franks et al. (2013) found that change in C<sub>a</sub> concentration changes the rates of carboxylation by Rubisco (in C<sub>3</sub> plants) and PEP carboxylase (in C<sub>4</sub> plants); each of these enzymes has a crucial limiting step in the photosynthetic pathway. An initial increase in  $P_n$  (less pronounced in C<sub>4</sub> plants) at or above the ambient C<sub>a</sub> concentration occurs because of the unique CO<sub>2</sub>-concentrating mechanism associated with C<sub>4</sub> photosynthesis (Ghannoum et al., 1997; von Caemmerer and Farquhar, 1999). In our study, we



further explored (i) the potential limiting factors of  $P_n$  when C<sub>3</sub> and C<sub>4</sub> plants were grown under condition of NH<sub>4</sub><sup>+</sup>-N nutrition, and (ii) the way in which changes in  $C_a$  concentration affected the potential NH<sub>4</sub><sup>+</sup> tolerance of C<sub>3</sub> and C<sub>4</sub> plants.

### Impaired Electron Transfer Associated With NH<sub>4</sub><sup>+</sup> Inhibited Photosynthesis

Under atmospheric CO<sub>2</sub> conditions, the carboxylation ability of Rubisco is the key factor limiting C<sub>3</sub> photosynthesis (Li et al., 2009; Carmo-Silva et al., 2015).  $V_{cmax}$ , which represents

the apparent Rubisco activity *in vivo* (Long and Bernacchi, 2003), increases with increasing CO<sub>2</sub> concentration (Jordan and Ogren, 1984). We found that both wheat and maize plants had lower  $g_s$  and  $V_{cmax}$  values under AN than under the other two N treatments, but  $C_i$  values were elevated under AN (Figure 3). Early CO<sub>2</sub> enrichment experiments using crops and tree saplings demonstrated that  $g_s$  was generally reduced by elevated CO<sub>2</sub> concentrations; we noted a similar phenomenon in wheat (Figure 3) (Yong et al., 1997; Medlyn et al., 2001). In contrast, the  $C_i$  and  $C_s$  of maize changed less with increases in  $C_a$ , regardless of the type of N nutrition. Li et al. (2015) suggested

**TABLE 3** | *F*-values in two-way ANOVA analysis of *F<sub>v</sub>/F<sub>m</sub>*,  $\Phi_{PSII}$ , NPQ and *qL* in newly expanded leaves of C<sub>3</sub> wheat and C<sub>4</sub> maize seedlings after 21 days of treatment with different N-sources.

Species	Source	df	<i>F<sub>v</sub>/F<sub>m</sub></i>		$\Phi_{PSII}$		NPQ		<i>qL</i>	
			Squares sum ( $\times 10^{-3}$ )	<i>F</i> -value	Squares sum ( $\times 10^{-3}$ )	<i>F</i> -value	Squares sum ( $\times 10^{-3}$ )	<i>F</i> -value	Squares sum ( $\times 10^{-3}$ )	<i>F</i> -value
Wheat	N	2	73(72.3)	11450**	102(86.4)	510**	1768(98.1)	1485**	326(81.7)	1753**
	CO <sub>2</sub>	2	9(8.9)	1369**	6(5.1)	29**	5(0.2)	4*	22(5.5)	117**
	N $\times$ CO <sub>2</sub>	4	19(18.8)	1478**	6(5.1)	15**	6(0.5)	3*	47(11.8)	127**
	Error	40	0(0.0)		4(3.4)		24(0.9)		4(1.0)	
Maize	N	2	57(96.6)	478**	189(96.7)	1013**	1671(98.4)	2249**	564(98.8)	2277**
	CO <sub>2</sub>	2	0(0.0)	0 ns	1(0.5)	4*	4(0.2)	5*	2(0.4)	6**
	N $\times$ CO <sub>2</sub>	4	0(0.0)	1 ns	1(0.5)	2 ns	8(0.5)	6**	0(0.0)	1 ns
	Error	40	2(3.4)		4(2.1)		15(0.9)		5(0.9)	

*N* refers to the three nitrogen-forms effect; CO<sub>2</sub> refers to the three CO<sub>2</sub> levels effect; N  $\times$  CO<sub>2</sub> refers to nitrogen-form  $\times$  CO<sub>2</sub> levels interaction effects. Values in brackets following the sum of squares for variables indicate the percentage (%) of given variation to total variation. \* and \*\* indicate significant at 0.05 and 0.01 level, respectively. *df* refers to the degree of freedom. ns means no significant difference.

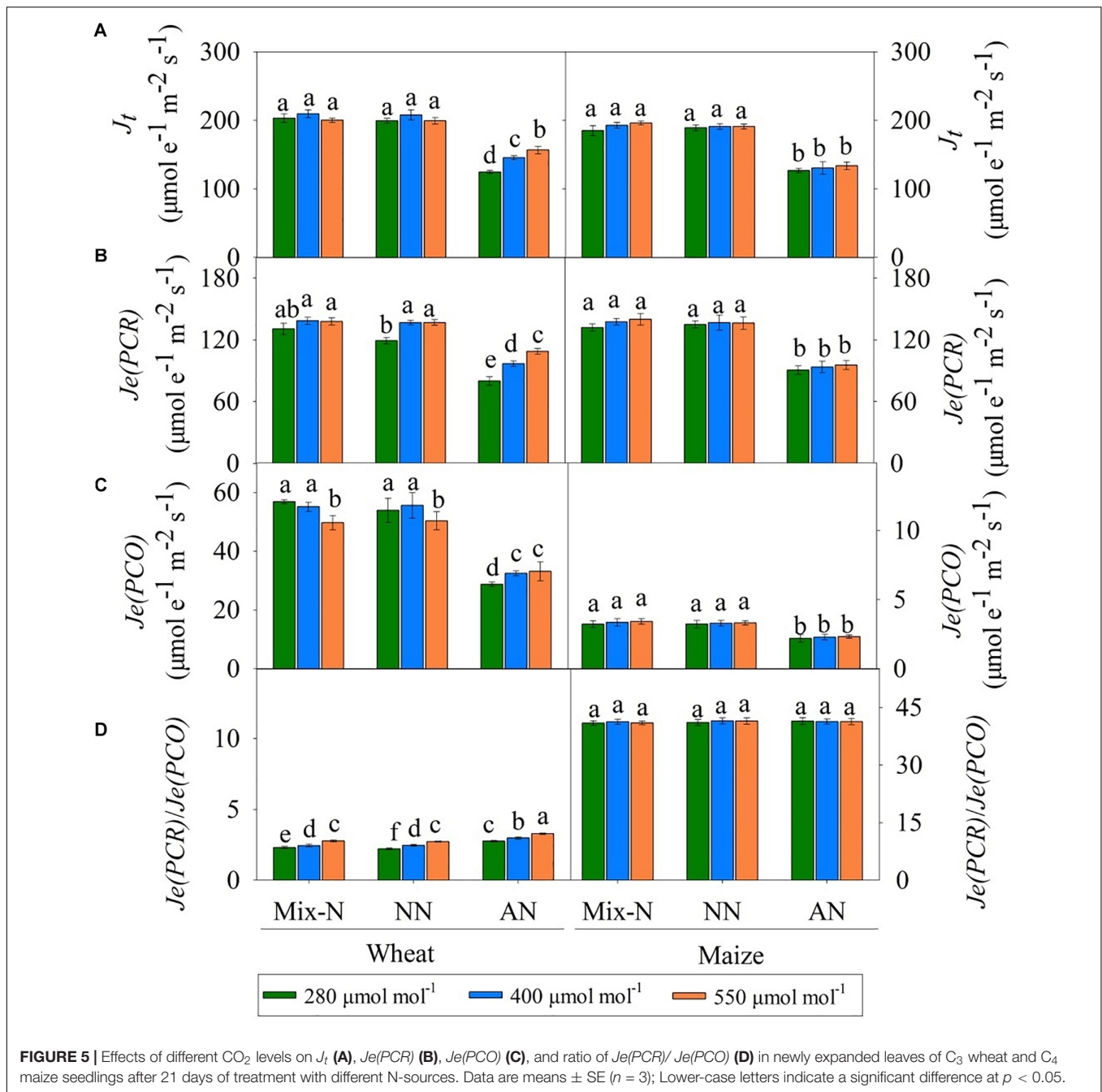
that the increases in *C<sub>i</sub>* may result from decreases in the rate of the photosynthetic dark CO<sub>2</sub> reduction when *g<sub>s</sub>* is reduced in C<sub>3</sub> plants.

Under ambient conditions, 44% of the absorbed light at peak PPFD was used for photosynthetic electron transport (25% for CO<sub>2</sub> fixation, 19% for photorespiration), and the remaining 56% was dissipated by chlorophyll fluorescence and thermal energy generation (Demmig-Adams and Adams, 1992). The balance between photosynthetic electron harvesting and transport within the chloroplasts is important for CO<sub>2</sub> assimilation based on the Calvin cycle (Demmig-Adams et al., 1989; Fryer et al., 1998; Shikanai, 2011). We found that *F<sub>v</sub>/F<sub>m</sub>*,  $\Phi_{PSII}$ , *qL* and *J<sub>t</sub>* were reduced under conditions of NH<sub>4</sub><sup>+</sup> nutrition (Figures 4A–C, 5A), indicating that the energy available for CO<sub>2</sub> assimilation was limited. Similar responses under conditions of NH<sub>4</sub><sup>+</sup> nutrition were reported by Johnson et al. (2011), where the photosynthetic electron transport chain was interrupted on the PSII side. The oxygen-evolving complex of PSII may be a direct target of NH<sub>4</sub><sup>+</sup>, causing a marked decline in photosynthesis (Drath et al., 2008). We found significant reductions in *J<sub>max</sub>*,  $\Phi_{PSII}$  and *J<sub>t</sub>* for both wheat and maize (Figures 3, 4B, 5A); the reductions for maize were especially marked, and led to deficiencies in NADPH and ATP availability for CO<sub>2</sub> assimilation (Gao et al., 2018). Cousins and Bloom (2003) suggested that NO<sub>3</sub><sup>-</sup> assimilation increases linear electron transfer and alleviates the photosynthetic ATP limitation in maize. In NH<sub>4</sub><sup>+</sup>-fed plants, the inadequate energy supply for CO<sub>2</sub> carboxylation may be a result of interruptions in the electron transport chain (Wang et al., 2019). With an impaired PSII, plants have a reduced capacity to dissipate excitation energy through *qL*, resulting in a surplus of light energy (Kim and Apel, 2013). We found that NPQ increased in both species (Figure 4D) via a process involving the scavenging of excess light energy through heat dissipation under conditions of NH<sub>4</sub><sup>+</sup> nutrition. This finding was consistent with a previous report showing that plants can dissipate excess excitation energy in the form of heat through NPQ when they encountered abiotic stresses (Demmig-Adams and Adams, 1992).

### Higher C<sub>a</sub> Enhanced CO<sub>2</sub> Assimilation, Which Provided Additional C Skeletons for NH<sub>4</sub><sup>+</sup> Assimilation in C<sub>3</sub> Plants

Under AN, the *J<sub>max</sub>*,  $\Phi_{PSII}$  and *J<sub>t</sub>* values of wheat increased with increasing CO<sub>2</sub> concentration (Figures 3, 4B, 5A), indicating that the interruption in electron transport can be offset by higher CO<sub>2</sub> concentration; these parameters did not differ significantly for maize grown under different CO<sub>2</sub> levels. At low atmospheric CO<sub>2</sub> levels, Rubisco utilizes both CO<sub>2</sub> and O<sub>2</sub> (Edwards et al., 2010). The process of uptaking O<sub>2</sub> leads to photorespiration, resulting in net losses of  $\leq 40\%$  of photosynthetic carbon under present day CO<sub>2</sub> levels of 400  $\mu\text{mol mol}^{-1}$  (Andrews and Lorimer, 1978; Sage, 2004; Bloom, 2015). C<sub>4</sub> photosynthesis suppresses photorespiration by concentrating CO<sub>2</sub> internally (Andrews and Lorimer, 1978; Ehleringer et al., 1991). Conversely, higher C<sub>a</sub> increases the CO<sub>2</sub> assimilation of C<sub>3</sub> plants and thereby inhibiting photorespiration; C<sub>4</sub> plants do not respond in this way (Andrews and Lorimer, 1978). We found that the *C<sub>i</sub>* and *C<sub>c</sub>* values of wheat under AN increased significantly with increased C<sub>a</sub>, leading to increases in *Je(PCR)*, whereas *Je(PCO)* did not change significantly (Figure 5D). As a result, the *Je(PCR)/Je(PCO)* ratio increased with increasing CO<sub>2</sub> concentration under AN (Figure 5C). These findings indicated that the electron flux to CO<sub>2</sub> assimilation was increased at higher CO<sub>2</sub> concentrations, which may compensate for the decrease in electron transport ability seen under AN, thereby sustaining carbon assimilation. In maize, there were no significant differences in *C<sub>i</sub>*, *C<sub>c</sub>* or *Je(PCR)/Je(PCO)* by CO<sub>2</sub> level on day 21 of the experiment (Figures 2, 5D).

Bloom et al. (2010) and Bloom (2015) found that (i) elevated CO<sub>2</sub> inhibits nitrite (NO<sub>2</sub><sup>-</sup>) transport into chloroplasts, (ii) the chloroplast stroma compete for reduced ferredoxin (Fdr), and (iii) elevated CO<sub>2</sub> levels decrease photorespiration, thereby inhibiting shoot NO<sub>3</sub><sup>-</sup> assimilation in C<sub>3</sub> plants under elevated CO<sub>2</sub> concentrations. In contrast, the first carboxylation reaction in the C<sub>4</sub> carbon fixation pathway generates ample quantities of malate and NADH in the cytoplasm of mesophyll cells.



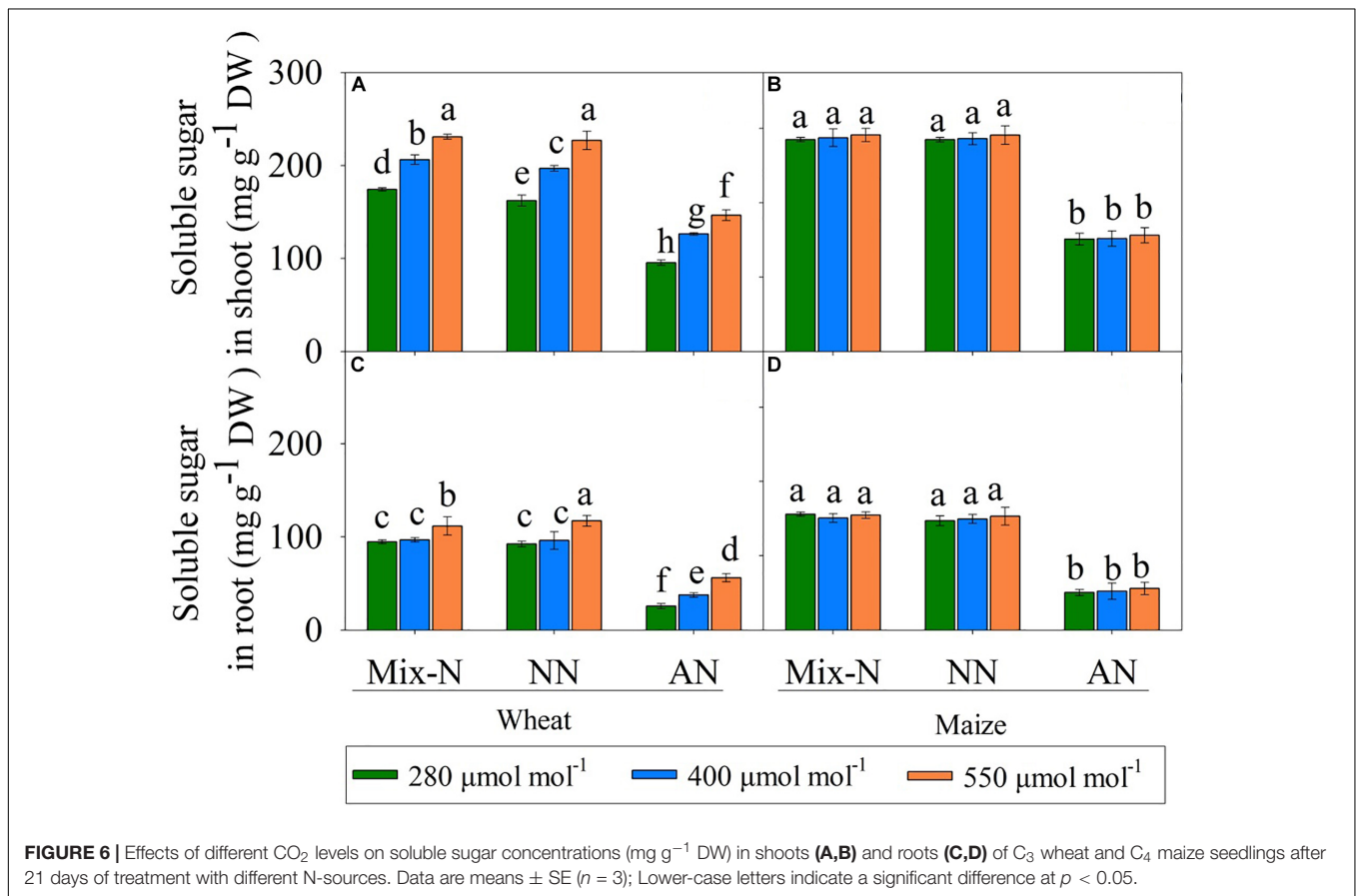
This explains adequately the CO<sub>2</sub>-independent shoot NO<sub>3</sub><sup>-</sup> assimilation in C<sub>4</sub> plants (Bloom et al., 2010). However, since N assimilation occurs rapidly when NH<sub>4</sub><sup>+</sup> is the sole source of N nutrition, an adequate C skeleton supply for NH<sub>4</sub><sup>+</sup> assimilation is required to facilitate general physiological homeostasis under elevated NH<sub>4</sub><sup>+</sup> concentrations (Ariz et al., 2013). Therefore, the carbohydrate status of plant tissues has an important role in the transition and adaptation to AN nutrition. A shortage of carbon assimilation for NH<sub>4</sub><sup>+</sup> form has been associated with a reduced level of soluble sugars in NH<sub>4</sub><sup>+</sup>-grown plants (Setien et al., 2013). We found

a significant decrease in the soluble sugar concentration in both species, especially in roots, under AN and ambient CO<sub>2</sub> conditions (Figure 6). With increasing C<sub>a</sub>, an increase in soluble sugar concentration and a decrease in free NH<sub>4</sub><sup>+</sup> concentration occurred in wheat, possibly because of an increase in CO<sub>2</sub> photosynthetic capacity (Ariz et al., 2010, 2013). Therefore, in wheat, an increased P<sub>n</sub> under AN, which was driven by elevated C<sub>a</sub> levels, increased the supply of carbon skeleton for NH<sub>4</sub><sup>+</sup> assimilation, which in turn reduced the NH<sub>4</sub><sup>+</sup> concentrations and thereby ameliorating the NH<sub>4</sub><sup>+</sup> stress.

**TABLE 4** | *F*-values in two-way ANOVA analysis of *J<sub>t</sub>*, *Je(PCR)*, *Je(PCO)*, and ratio of *Je(PCR)/Je(PCO)* in newly expanded leaves of C<sub>3</sub> wheat and C<sub>4</sub> maize seedlings after 21 days of treatment with different N-sources.

Species	Source	df	<i>J<sub>t</sub></i>		<i>Je(PCR)</i>		<i>Je(PCO)</i>		<i>Je(PCR)/Je(PCO)</i>	
			Squares sum (×10 <sup>3</sup> )	<i>F</i> -value	Squares sum (×10 <sup>3</sup> )	<i>F</i> -value	Squares sum	<i>F</i> -value	Squares sum	<i>F</i> -value
Wheat	N	2	44.5(90.5)	931**	17.6 (79.7)	719**	5885 (90.1)	363.3**	3.29(57.1)	454.2**
	CO <sub>2</sub>	2	1.4(2.9)	30**	3.2 (14.5)	130**	104 (1.6)	6.4**	2.30 (40.0)	318.0**
	N × CO <sub>2</sub>	4	2.3(4.6)	23**	0.8 (3.5)	15**	219 (3.4)	6.7**	0.22 (0.4)	1.5 ns
	Error	40	1.0(1.9)		0.5 (2.2)		323 (5.0)		0.15 (2.5)	
Maize	N	2	43.9 (96.5)	838**	22.2 (95.2)	529**	123 (90.5)	225.9**	0.97(6.1)	1.4 ns
	CO <sub>2</sub>	2	0.4 (0.9)	7**	0.2 (0.9)	5**	0 (1.3)	3.3*	0.46 (2.9)	0.6 ns
	N × CO <sub>2</sub>	4	0.1 (0.3)	1 ns	0.1 (0.3)	1 ns	0 (0.1)	0.1 ns	0.64 (4.1)	0.4 ns
	Error	40	1.0(2.3)		0.8 (3.6)		1 (8.0)		13.64 (86.8)	

*N* refers to the three nitrogen-forms effect; *CO*<sub>2</sub> refers to the three *CO*<sub>2</sub> levels effect; *N* × *CO*<sub>2</sub> refers to nitrogen-form × *CO*<sub>2</sub> levels interaction effects. Values in brackets following the sum of squares for variables indicate the percentage (%) of given variation to total variation. \* and \*\* indicate significant at 0.05 and 0.01 level, respectively. *df* refers to the degree of freedom. ns means no significant difference.



## CONCLUSION

In conclusion, under ambient CO<sub>2</sub> conditions and AN nutrition, electron transport was reduced in both the C<sub>3</sub> wheat and C<sub>4</sub> maize plants, leading to a suppression of photosynthetic carbon assimilation. In wheat growing under elevated atmospheric CO<sub>2</sub> concentrations (*C<sub>a</sub>*), increased *C<sub>i</sub>* and *C<sub>c</sub>* values improved electron flux to CO<sub>2</sub> assimilation rather than to photorespiration, thus sustaining photosynthesis

and alleviating NH<sub>4</sub><sup>+</sup>-induced stress. In contrast, elevated *C<sub>a</sub>* had a negligible effect on *C<sub>i</sub>* and *C<sub>s</sub>* in maize and, consequently, minor effects on photosynthesis. Therefore, future increases in atmospheric *C<sub>a</sub>* should provide C<sub>3</sub> plants with more opportunities to use NH<sub>4</sub><sup>+</sup> rather than relying on NO<sub>3</sub><sup>-</sup> as a source of N fertilizers for crop production. Analyses using molecular biology and mutants to explain the possible physiological mechanisms in NH<sub>4</sub><sup>+</sup> tolerance of crop cultivars.

## DATA AVAILABILITY STATEMENT

All datasets generated for this study are included in the manuscript/**Supplementary Material**.

## AUTHOR CONTRIBUTIONS

FW and XH conceived the original screening and research plans. FW, JG, and XH supervised the experiments. FW performed most of the experiments, conceived the project, and wrote the article with salient contributions from all the authors in specific areas. FW, JG, JY, QW, JM, and XH supervised and completed the writing. All authors contributed to the article and approved the submitted version.

## FUNDING

This work was supported by the 100 Talents Program of Chongqing (20710940) and the World-Class Biological Science

Discipline Development Program at the Southwest University, China (100030/2120054019), the Chinese Postdoctoral Science Foundation (2017M622948) and the Chongqing Postdoctoral Science Foundation (Xm2017147), and Key R & D project of Zhejiang Province “R & D and application of green, safe and efficient fertilizers” (2020R20A50B01).

## ACKNOWLEDGMENTS

The authors would like to thank Professor Hans Lambers (School of Biological Sciences, University of Western Australia) for guidance in writing the manuscript.

## SUPPLEMENTARY MATERIAL

The Supplementary Material for this article can be found online at: <https://www.frontiersin.org/articles/10.3389/fpls.2020.537443/full#supplementary-material>

## REFERENCES

- Anderson, L. J., Maherali, H., Johnson, H. B., Polley, H. W., and Jackson, R. B. (2001). Gas exchange and photosynthetic acclimation over subambient to elevated CO<sub>2</sub> in a C<sub>3</sub>-C<sub>4</sub> grassland. *Global Change Biol.* 7, 693–707. doi: 10.1046/j.1354-1013.2001.00438.x
- Andrews, T. J., and Lorimer, G. H. (1978). Photorespiration—still still unavoidable? *FEBS Lett.* 90, 1–9. doi: 10.1016/0014-5793(78)80286-5
- Aranjuelo, I., Pardo, A., Biel, C., Save, R., Azcon-Bieto, J., and Nogues, S. (2009). Leaf carbon management in slow-growing plants exposed to elevated CO<sub>2</sub>. *Global Change Biol.* 15, 97–109. doi: 10.1111/j.1365-2486.2008.01829.x
- Ariz, I., Artola, E., Asensio, A. C., Cruchaga, S., Aparicio-Tejo, P. M., and Moran, J. F. (2011). High irradiance increases NH<sub>4</sub><sup>+</sup> tolerance in *Pisum sativum*: higher carbon and energy availability improve ion balance but not N assimilation. *J. Plant Physiol.* 168, 1009–1015. doi: 10.1016/j.jplph.2010.11.022
- Ariz, I., Asensio, A. C., Zamarreno, A. M., Garcia-Mina, J. M., Aparicio-Tejo, P. M., and Moran, J. F. (2013). Changes in the C/N balance caused by increasing external ammonium concentrations are driven by carbon and energy availabilities during ammonium nutrition in pea plants: the key roles of asparagine synthetase and anaplerotic enzymes. *Physiol. Plant.* 148, 522–537. doi: 10.1111/j.1399-3054.2012.01712.x
- Ariz, I., Esteban, R., García-Plazaola, J. I., Becerril, J. M., Aparicio-Tejo, P. M., and Moran, J. F. (2010). High irradiance induces photoprotective mechanisms and a positive effect on NH<sub>4</sub><sup>+</sup> stress in *Pisum sativum* L. *J. Plant Physiol.* 167, 1038–1045. doi: 10.1016/j.jplph.2010.02.014
- Balkos, K. D., Britto, D. T., and Kronzucker, H. J. (2010). Optimization of ammonium acquisition and metabolism by potassium in rice (*Oryza sativa* L. cv. IR-72). *Plant Cell Environ.* 33, 23–34.
- Bloom, A. J. (2015). Photorespiration and nitrate assimilation: a major intersection between plant carbon and nitrogen. *Photosynth. Res.* 123, 117–128. doi: 10.1007/s11120-014-0056-y
- Bloom, A. J., Burger, M., Asensio, J. S. R., and Cousins, A. B. (2010). Carbon dioxide enrichment inhibits nitrate assimilation in wheat and *Arabidopsis*. *Science* 328, 899–903. doi: 10.1126/science.1186440
- Bloom, A. J., Burger, M., Kimball, B. A., and Pinter, P. J. (2014). Nitrate assimilation is inhibited by elevated CO<sub>2</sub> in field-grown wheat. *Nat. Clim. Chang.* 4:477. doi: 10.1038/nclimate2183
- Bloom, A. J., Smart, D. R., Nguyen, D. T., and Searles, P. S. (2002). Nitrogen assimilation and growth of wheat under elevated carbon dioxide. *Proc. Natl. Acad. Sci. U. S. A.* 99, 1730–1735. doi: 10.1073/pnas.022627299
- Britto, D. T., and Kronzucker, H. J. (2002). NH<sub>4</sub><sup>+</sup> toxicity in higher plants: a critical review. *J. Plant Physiol.* 159, 567–584. doi: 10.1078/0176-1617-0774
- Carmo-Silva, E., Scales, J. C., Madgwick, P. J., and Parry, M. A. (2015). Optimizing Rubisco and its regulation for greater resource use efficiency. *Plant, Cell Environ.* 38, 1817–1832. doi: 10.1111/pce.12425
- Conn, S. J., Hocking, B., Dayod, M., Xu, B., Athman, A., Henderson, S., et al. (2013). Protocol: optimising hydroponic growth systems for nutritional and physiological analysis of *Arabidopsis thaliana* and other plants. *Plant Methods* 9:4. doi: 10.1186/1746-4811-9-4
- Coskun, D., Britto, D. T., Shi, W., and Kronzucker, H. J. (2017). Nitrogen transformations in modern agriculture and the role of biological nitrification inhibition. *Nat. Plants* 3:17074.
- Cousins, A. B., and Bloom, A. J. (2003). Influence of elevated CO<sub>2</sub> and nitrogen nutrition on photosynthesis and nitrate photoreduction in maize (*Zea mays* L.). *Plant Cell Environ.* 26, 1525–1530. doi: 10.1046/j.1365-3040.2003.01075.x
- Demmig-Adams, B., and Adams, W. I. I. (1992). Photoprotection and other responses of plants to high light stress. *Ann. Rev. Plant Biol.* 43, 599–626. doi: 10.1146/annurev.pp.43.060192.003123
- Demmig-Adams, B., Winter, K., Krüger, A., and Czygan, F. C. (1989). Light response of CO<sub>2</sub> assimilation, dissipation of excess excitation energy, and zeaxanthin content of sun and shade leaves. *Plant Physiol.* 90, 881–886. doi: 10.1104/pp.90.3.881
- Dier, M., Meinen, R., Erbs, M., Kollhorst, L., Baillie, C. K., Kaufholdt, D., et al. (2018). Effects of free air carbon dioxide enrichment (FACE) on nitrogen assimilation and growth of winter wheat under nitrate and ammonium fertilization. *Global Change Biol.* 24, e40–e54.
- Drath, M., Kloft, N., Batschauer, A., Marin, K., Novak, J., and Forchhammer, K. (2008). Ammonia triggers photodamage of photosystem II in the cyanobacterium *Synechocystis* sp. strain PCC 6803. *Plant Physiol.* 147, 206–215. doi: 10.1104/pp.108.117218
- Edwards, E. J., Osborne, C. P., Strömberg, C. A., Smith, S. A., and Consortium, C. G. (2010). The origins of C<sub>4</sub> grasslands: integrating evolutionary and ecosystem science. *Science* 328, 587–591. doi: 10.1126/science.1177216
- Ehleringer, J. R., Sage, R. F., Flanagan, L. B., and Pearcy, R. W. (1991). Climate change and the evolution of C<sub>4</sub> photosynthesis. *Trends Ecol. Evol.* 6:95. doi: 10.1016/0169-5347(91)90183-x
- Farquhar, G. D., von Caemmerer, ., and Berry, J. (1980). A biochemical model of photosynthetic CO<sub>2</sub> assimilation in leaves of C<sub>3</sub> species. *Planta* 149, 78–90. doi: 10.1007/bf00386231

- Fernández-Crespo, E., Camañes, G., and García-Agustín, P. (2012). Ammonium enhances resistance to salinity stress in citrus plants. *J. Plant Physiol.* 169, 1183–1191. doi: 10.1016/j.jplph.2012.04.011
- Franks, P. J., Adams, M. A., Amthor, J. S., Barbour, M. M., Berry, J. A., Ellsworth, D. S., et al. (2013). Sensitivity of plants to changing atmospheric CO<sub>2</sub> concentration: from the geological past to the next century. *New Phytol.* 197, 1077–1094. doi: 10.1111/nph.12104
- Fryer, M. J., Andrews, J. R., Oxborough, K., Blowers, D. A., and Baker, N. R. (1998). Relationship between CO<sub>2</sub> assimilation, photosynthetic electron transport, and active O<sub>2</sub> metabolism in leaves of maize in the field during periods of low temperature. *Plant Physiol.* 116, 571–580. doi: 10.1104/pp.116.2.571
- Gao, J., Wang, F., Sun, J., Tian, Z., Hu, H., Jiang, S., et al. (2018). Enhanced Rubisco activation associated with maintenance of electron transport alleviates inhibition of photosynthesis under low nitrogen conditions in winter wheat seedlings. *J. Exp. Botany* 69, 5477–5488.
- Genty, B., Briantais, J. M., and Baker, N. R. (1989). The relationship between the quantum yield of photosynthetic electron transport and quenching of chlorophyll fluorescence. *Biochim. Biophys. Acta Gen. Subj.* 990, 87–92. doi: 10.1016/s0304-4165(89)80016-9
- Ghannoum, O., Caemmerer, S., Ziska, L. H., and Conroy, J. P. (2000). The growth response of C<sub>4</sub> plants to rising atmospheric CO<sub>2</sub> partial pressure: a reassessment. *Plant Cell Environ.* 23, 931–942. doi: 10.1046/j.1365-3040.2000.00609.x
- Ghannoum, O., von Caemmerer, S., Barlow, E. W., and Conroy, J. P. (1997). The effect of CO<sub>2</sub> enrichment and irradiance on the growth, morphology and gas exchange of a C<sub>3</sub> (*Panicum laxum*) and a C<sub>4</sub> (*Panicum antidotale*) grass. *Funct. Plant Biol.* 24, 407–407. doi: 10.1071/pp96077\_co
- Gong, P., Liang, L., and Zhang, Q. (2011). China must reduce fertilizer use too. *Nature* 473, 284–285. doi: 10.1038/473284e
- Hatch, M. D., and Slack, C. R. (1966). Photosynthesis by sugar-cane leaves: a new carboxylation reaction and the pathway of sugar formation. *Biochem. J.* 101, 103–111. doi: 10.1042/bj1010103
- IPCC (2007). *Agriculture: Contribution of Working Group III to the Fourth Assessment Report of the Intergovernmental Panel on Climate Change*, eds B. Metz, O. R. Davidson, P. R. Bosch, R. Dave, and L. A. Meyer (Cambridge, New York, NY: Cambridge University Press), 497–540.
- IPCC (2013). *Climate Change 2013: The Physical Science Basis. Contribution of Working Group I to the Fifth Assessment Report of the Intergovernmental Panel on Climate Change*, eds T. F. Stocker, D. Qin, G. K. Plattner, M. Tignor, S. K. Allen, J. Boschung, et al. (Cambridge, New York, NY: Cambridge University Press).
- Johnson, M. P., Goral, T. K., Duffy, C. D., Brain, A. P., Mullineaux, C. W., and Ruban, A. V. (2011). Photoprotective energy dissipation involves the reorganization of photosystem II light-harvesting complexes in the grana membranes of spinach chloroplasts. *Plant Cell* 23, 1468–1479. doi: 10.1105/tpc.110.081646
- Jordan, D. B., and Ogren, W. L. (1984). The CO<sub>2</sub>/O<sub>2</sub> specificity of ribulose 1, 5-bisphosphate carboxylase/oxygenase. *Planta* 161, 308–313.
- Kanemoto, K., Yamashita, Y., Ozawa, T., Imanishi, N., Nguyen, N. T., Suwa, R., et al. (2009). Photosynthetic acclimation to elevated CO<sub>2</sub> is dependent on N partitioning and transpiration in soybean. *Plant Sci.* 177, 398–403. doi: 10.1016/j.plantsci.2009.06.017
- Kim, C., and Apel, K. (2013). Singlet oxygen-mediated signaling in plants: moving from flu to wild type reveals an increasing complexity. *Photosynth. Res.* 116, 455–464. doi: 10.1007/s11120-013-9876-4
- Kramer, D. M., Johnson, G., Kiirats, O., and Edwards, G. E. (2004). New fluorescence parameters for the determination of QA redox state and excitation energy fluxes. *Photosynth. Res.* 79:209. doi: 10.1023/b:pres.0000015391.99477.0d
- Kühlbrandt, W., Wang, D. N., and Fujiyoshi, Y. (1994). Atomic model of plant light-harvesting complex by electron crystallography. *Nature* 367, 614–621. doi: 10.1038/367614a0
- Leakey, A. D., Uribealrrea, M., Ainsworth, E. A., Naidu, S. L., Rogers, A., Ort, D. R., et al. (2006). Photosynthesis, productivity, and yield of maize are not affected by open-air elevation of CO<sub>2</sub> concentration in the absence of drought. *Plant Physiol.* 140, 779–790. doi: 10.1104/pp.105.073957
- Li, B., Shi, W., and Su, Y. (2011). The differing responses of two *Arabidopsis* ecotypes to ammonium are modulated by the photoperiod regime. *Acta Physiol. Plant.* 33, 325–334. doi: 10.1007/s11738-010-0551-5
- Li, H., Wang, Y., Xiao, J., and Xu, K. (2015). Reduced photosynthetic dark reaction triggered by ABA application increases intercellular CO<sub>2</sub> concentration, generates H<sub>2</sub>O<sub>2</sub> and promotes closure of stomata in ginger leaves. *Environ. Exp. Bot.* 113, 11–17. doi: 10.1016/j.envexpbot.2015.01.002
- Li, Y., Gao, Y., Xu, X., Shen, Q., and Guo, S. (2009). Light-saturated photosynthetic rate in high-nitrogen rice (*Oryza sativa* L.) leaves is related to chloroplastic CO<sub>2</sub> concentration. *J. Exp. Bot.* 60, 2351–2360. doi: 10.1093/jxb/erp127
- Lloyd, J., and Farquhar, G. D. (1996). The CO<sub>2</sub> dependence of photosynthesis, plant growth responses to elevated atmospheric CO<sub>2</sub> concentrations and their interaction with soil nutrient status. I. General principles and forest ecosystems. *Funct. Ecol.* 10, 4–32. doi: 10.2307/2390258
- Long, S. P., and Bernacchi, C. J. (2003). Gas exchange measurements, what can they tell us about the underlying limitations to photosynthesis? Procedures and sources of error. *J. Exp. Bot.* 54, 2393–2401. doi: 10.1093/jxb/erg262
- Medlyn, B., Barton, C. V. M., Broadmeadow, M. S. J., Ceulemans, R., De Angelis, P., Forstreuter, M., et al. (2001). Stomatal conductance of forest species after long-term exposure to elevated CO<sub>2</sub> concentration: a synthesis. *New Phytol.* 149, 247–264. doi: 10.1046/j.1469-8137.2001.00028.x
- Mehrer, I., and Mohr, H. (1989). Ammonium toxicity: description of the syndrome in *Sinapis alba* and the search for its causation. *Physiol. Plant.* 77, 545–554. doi: 10.1111/j.1399-3054.1989.tb05390.x
- Miller, A. J., and Cramer, M. D. (2005). Root nitrogen acquisition and assimilation. *Plant Soil* 274, 1–36. doi: 10.1007/1-4020-4099-7\_1
- Nguyen, N. T., McInturf, S. A., and Mendoza-Cózatl, D. G. (2016). Hydroponics: a versatile system to study nutrient allocation and plant responses to nutrient availability and exposure to toxic elements. *J. Vis. Exp.* 113:e54317.
- Onoda, Y., Hikosaka, K., and Hirose, T. (2004). Allocation of nitrogen to cell walls decreases photosynthetic nitrogen-use efficiency. *Funct. Ecol.* 18, 419–425. doi: 10.1111/j.0269-8463.2004.00847.x
- Owensby, C. E., Ham, J. M., Knapp, A. K., and Auen, L. M. (1999). Biomass production and species composition change in a tallgrass prairie ecosystem after long-term exposure to elevated atmospheric CO<sub>2</sub>. *Global Change Biol.* 5, 497–506. doi: 10.1046/j.1365-2486.1999.00245.x
- Richter, J., and Roelcke, M. (2000). The N-cycle as determined by intensive agriculture—examples from central Europe and China. *Nutr. Cycl. Agroecosyst.* 57, 33–46.
- Robredo, A., Pérez-López, U., Miranda-Apodaca, J., Lacuesta, M., Mena-Petite, A., and Muñoz-Rueda, A. (2011). Elevated CO<sub>2</sub> reduces the drought effect on nitrogen metabolism in barley plants during drought and subsequent recovery. *Environ. Exp. Bot.* 71, 399–408. doi: 10.1016/j.envexpbot.2011.02.011
- Sage, R. F. (2004). The evolution of C<sub>4</sub> photosynthesis. *New Phytol.* 161, 341–370.
- Setien, I., Fuertes-Mendizabal, T., Gonzalez, A., Aparicio-Tejo, P. M., Gonzalez-Murua, C., Gonzalez-Moro, M. B., et al. (2013). High irradiance improves ammonium tolerance in wheat plants by increasing N assimilation. *J. Plant Physiol.* 170, 758–771. doi: 10.1016/j.jplph.2012.12.015
- Shikanai, T. (2011). Regulation of photosynthetic electron transport. *Biochim. Biophys. Acta* 1807, 375–383.
- von Caemmerer, S., and Farquhar, G. D. (1999). “The modelling of C<sub>4</sub> photosynthesis,” in *The Biology of C<sub>4</sub> Photosynthesis*, ed. R. M. Sage (New York, NY: Academic Press), 173–211.
- Wang, F., Gao, J., Liu, Y., Tian, Z., Muhammad, A., Zhang, Y., et al. (2016a). Higher ammonium transamination capacity can alleviate glutamate inhibition on winter wheat (*Triticum aestivum* L.) root growth under high ammonium stress. *PLoS One* 11:e0160997. doi: 10.1371/journal.pone.0160997
- Wang, F., Gao, J., Shi, S., He, X., and Dai, T. (2019). Impaired electron transfer accounts for the photosynthesis inhibition in wheat seedlings (*Triticum aestivum* L.) subjected to ammonium stress. *Physiol. Plant.* 167, 159–172. doi: 10.1111/ppl.12878
- Wang, F., Gao, J., Tian, Z., Liu, Y., Abid, M., Jiang, D., et al. (2016b). Adaptation to rhizosphere acidification is a necessary prerequisite for wheat (*Triticum aestivum* L.) seedling resistance to ammonium stress. *Plant Physiol. Biochem.* 108, 447–455. doi: 10.1016/j.plaphy.2016.08.011

- Xing, G., and Zhu, Z. (2000). An assessment of N loss from agricultural fields to the environment in China. *Nutr. Cycl. Agroecosyst.* 57, 67–73.
- Xu, G., Fan, X., and Miller, A. J. (2012). Plant nitrogen assimilation and use efficiency. *Ann. Rev. Plant Biol.* 63, 153–182. doi: 10.1146/annurev-arplant-042811-105532
- Yong, J. W. H., Letham, D. S., Wong, S. C., and Farquhar, G. D. (2010). Effects of root restriction on growth and associated cytokinin levels in cotton (*Gossypium hirsutum*). *Funct. Plant Biol.* 3, 974–984. doi: 10.1071/fp10009
- Yong, J. W. H., Wong, S. C., and Farquhar, G. D. (1997). Stomatal responses to changes in vapour pressure difference between leaf and air. *Plant Cell Environ.* 20, 1213–1216. doi: 10.1046/j.1365-3040.1997.d01-27.x
- Yong, J. W. H., Wong, S. C., Letham, D. S., Hocart, C. H., and Farquhar, G. D. (2000). Effects of elevated CO<sub>2</sub> and nitrogen nutrition on cytokinins in the xylem sap and leaves of cotton. *Plant Physiol.* 124, 767–780. doi: 10.1104/pp.124.2.767
- Zhou, Y. H., Yu, J. Q., Huang, L. F., and Nogues, S. (2004). The relationship between CO<sub>2</sub> assimilation, photosynthetic electron transport and water-water cycle in chill-exposed cucumber leaves under low light and subsequent recovery. *Plant Cell Environ.* 27, 1503–1514. doi: 10.1111/j.1365-3040.2004.01255.x

**Conflict of Interest:** The authors declare that the research was conducted in the absence of any commercial or financial relationships that could be construed as a potential conflict of interest.

Copyright © 2020 Wang, Gao, Yong, Wang, Ma and He. This is an open-access article distributed under the terms of the Creative Commons Attribution License (CC BY). The use, distribution or reproduction in other forums is permitted, provided the original author(s) and the copyright owner(s) are credited and that the original publication in this journal is cited, in accordance with accepted academic practice. No use, distribution or reproduction is permitted which does not comply with these terms.